Computer Modeling in Engineering & Sciences

Tech Science Press

https://doi.org/10.32604/cmes.2026.079763

ARTICLE

A Stochastic Multi-Objective Framework for Wind DG Allocation and Dynamic Reconfiguration: Minimizing Losses and Enhancing Reliability with an Improved Grey Wolf Optimizer

Ali S. Alghamdi*

Department of Electrical Engineering, College of Engineering, Majmaah University, Al-Majmaah, 11952, Saudi Arabia

*Corresponding Author: Ali S. Alghamdi. Email: aalghamdi@mu.edu.sa

Received: 27 January 2026; Accepted: 07 April 2026; Published: 27 April 2026

ABSTRACT: The integration of wind-based DG introduces significant variability and uncertainty into the operation of distribution networks, which complicates the planning and decision-making process. This paper presents a dual-objective stochastic optimization framework for the optimal allocation of wind DG, considering dynamic network reconfiguration across multiple loading conditions. Probabilistic modeling of wind speed is integrated using the Weibull distribution and the associated wind power uncertainty is discretized through a scenario-based point estimation method. Variability in load is accounted for by considering multiple loading levels, and the integrated uncertainty space is constructed as the Cartesian product of wind scenarios and load profiles. The optimization seeks to minimize the total energy losses together with the enhancement of reliability, quantified through the expected energy not supplied. For the solution of the complex, nonlinear, multi-objective problem, the Improved Multi-Objective Grey Wolf Optimizer (I-MGWO) is developed, including quasi-oppositional population seeding, adaptive stochastic coefficient strategy, and dynamic convex combination position update. Simulation results on the IEEE 33-bus system demonstrate that the proposed integrated strategy of simultaneous wind DG allocation and network reconfiguration gives synergistic improvements, yielding up to 55.7% reduction in energy losses, and a reduction of up to 61.4% in EENS over the base case. In both convergence speed and solution quality, I-MGWO consistently outperforms conventional algorithms and gives a robust and computationally efficient tool for distribution system planning under uncertainty.

KEYWORDS: Wind power generation; distributed generation allocation; active distribution network; network reconfiguration; uncertainty modeling; stochastic optimization; multi-objective optimization; reliability assessment; Grey Wolf Optimizer

1 Introduction

1.1 Background and Motivation

This is driving the widespread integration of renewable energy sources and places variable wind-based DG at the heart of contemporary distribution networks. Its inherent variability, however, is the source of significant uncertainty that complicates network planning and operation [1,2]. Independently, load demand varies temporally; together, these factors further increase operational difficulty [3]. Classic deterministic approaches to planning are poorly suited to this indeterminate environment, since it risks either inadequate asset utilization or actual constraint violation due to realistic variability [4].

Similarly, optimal wind DG allocation should reconcile competing objectives, such as minimizing energy losses to enhance efficiency and improving reliability, often measured via the Expected Energy Not

Supplied (EENS), to limit outage impacts. These objectives often conflict, hence requiring multi-objective optimization to find viable trade-offs. Moreover, the potential of DG is magnified when coordinated with network reconfiguration, a cost-effective strategy to adapt network topology to changing conditions. Despite their synergy, most studies optimize these elements in isolation, overlooking the compounded benefits of integrated planning. A comprehensive synthesis of these multi-objective planning challenges is provided by Al-Shamma'a et al. [5], who present a systematic review of optimization techniques, global insights, and smart grid implications for DG sizing and allocation. Their analysis of algorithmic trends and modeling innovations reinforces the importance of developing advanced metaheuristic approaches to address the increasing complexity of modern distribution systems.

Thus, the core challenge is to develop a stochastic multi-objective framework that simultaneously determines the optimal allocation of wind DG and dynamic network reconfiguration across multiple loading levels while accounting for uncertainties in both wind generation and load demand. This requires searching for a high-dimensional, constrained search space of discrete and continuous variables, which remains computationally demanding for conventional optimization methods [6,7].

1.2 Literature Review

In the context of distribution system performance, the driving force for DG integration is a major impetus. Optimizing key technical objectives, such as minimizing active power losses [3,8–11], has been one of the early and continuous areas of research. Improving voltage profiles, stability, and voltage deviation has also been widely investigated using various optimization frameworks for DG placement and sizing in distribution networks [8,9,12–15]. Several recent studies further explore advanced metaheuristic and evolutionary algorithms to enhance voltage stability and operational performance in both balanced and unbalanced systems [16–18].

In recent times, the scope has expanded toward economic and environmental considerations, thereby including other important objectives of multi-objective optimal planning, such as minimizing investment and operational costs [3,4,8,12]. These approaches increasingly incorporate techno-economic evaluations together with environmental and operational constraints to provide more practical DG planning strategies [15,19]. Additionally, reducing pollutant emissions and improving sustainability have been emphasized through advanced optimization techniques and renewable-based DG integration [20,21]. The review presented in [6] synthesizes these multi-objective planning challenges and underlines the inherent trade-offs that require more advanced optimization frameworks.

Another critical development is the transition from deterministic models to stochastic ones that consider genuine uncertainties. The intermittency of renewable DG, especially wind and solar, has become a key driver. Probabilistic models such as the Weibull distribution of wind speed and scenario-based approaches like the point estimation method to discretize this uncertainty for optimization have been undertaken [1,2]. Moreover, temporal variations in load are captured by time-varying loads [2] and multiple loading levels (e.g., high, medium, low) [3,22]. The incorporation of nonlinear, voltage dependent load models has also shown to have significant consequences on optimal DG sitting and sizing decisions [4]. This integration of generation and load uncertainty creates a more robust planning structure and is echoed in studies that put together these elements for a holistic uncertainty space [1,23–25].

The high-dimensional, non-linear, non-convex, and often multi-objective optimization problems emerging have, in turn, driven the development and application of lots of meta-heuristic algorithms. Conventional algorithms like GA [7,16] and PSO [8,9,11,15] are used broadly. This quest for better performance has welcomed and enhanced newer algorithms such as AOA [18], GWO along with its hybrid variants [8], SSA [2,24], and Jaya Algorithm [21]. In turn, a common thread is the modification of base algorithms

to transcend these simple variants' shortcomings, like premature convergence and/or poor population diversity. Enhancements include quasi-oppositional learning [20], hybrid strategies that combine different algorithms [8], and adaptive coefficient mechanisms as the most common proposals to improve exploration and exploitation capabilities and solution quality [17,20,26].

Given the synergies between different grid management tools, recent workplaces emphasis on integrated planning. Of note is that which considers the optimal allocation of DG and simultaneous network reconfiguration-the optimization of tie-switch status to minimize losses and improve voltage profiles for a range of different conditions [27] to exploit the flexibility of active distribution networks to maximize DG benefits. Further integration extends to coordinating DG with other devices, such as CBs [3,4,17], DSTATCOMs [14], SOPs [10], BESS [25,28] and AVRs [12]. Various studies, such as those by Elseify et al. [17] and the review by Kerur et al. [7], have underlined that coordinated planning gives better technical and economic results than optimizing each component separately.

The modern context of DG integration is represented by the paradigm of active distribution networks. Modern research incorporates active management schemes, such as coordinated voltage control and demand response (DR), to handle uncertainties and improve hosting capacity [25,28]. In addition to loss minimization, reliability assessment, quantified by metrics such as EENS, has become an important objective [1,13]. It has been demonstrated that strategic placement of DG, especially island-capable DG, significantly increases system reliability, since they provide local supply in case of upstream outages, a consideration of key importance in modern planning frameworks.

Recent studies by Cikan [29] focus on multi-objective solutions for optimizing unbalanced power distribution networks with reconfiguration. The results on the 37-bus system indicate that network reconfiguration alone can lead to substantial improvements in multiple technical and reliability criteria, thereby justifying the inclusion of reconfiguration as a decision variable in distribution system optimization problems. Alongside these planning-oriented solutions, operational tools such as Dynamic Thermal Line Rating (DTLR) and electric vehicle scheduling with Vehicle-to-Grid (V2G) capacity have been identified to make substantial contributions to the improvement of the reliability of wind-based networks by offering real-time flexibility to compensate for wind power variability in real-time [30]. While DTLR offers dynamic expansion of line capacities according to real-time weather conditions to mitigate congestion, and EVs offer distributed storage capacity to compensate for wind power variability, our framework proposes solutions to the underlying planning-oriented decisions of wind DG allocation and network reconfiguration, which form the infrastructure upon which such operational solutions can be effectively leveraged.

1.3 Identified Research Gaps and Contributions of This Work

Despite the vast amount of literature on DG allocation and network reconfiguration, some critical gaps still exist that this work aims to fill:

- Gap 1: Although some works have considered either the wind uncertainty or the load variability, few have built a comprehensive stochastic model that systematically combines probabilistic wind scenarios with different deterministic load levels via the Cartesian product. This is particularly important since the optimal network topology for high wind scenarios can be vastly different depending on whether it is aligned with peak or off-peak loading.
- Gap 2: While some works have addressed DG allocation and network reconfiguration in a sequential manner or with simplified coupling, the strong coupling between wind DG allocation and network reconfiguration for different load levels needs to be addressed in a simultaneous optimization manner. Moreover, instead of fixing the reconfiguration schemes for different load levels independently, which

is less representative of the flexibility of modern active distribution networks, this work adopts a more flexible approach.

- Gap 3: The integration of reliability as a key objective is still a challenge, and it is often addressed using simulation-based methods that are computationally expensive for metaheuristic search. There is a gap for the development of analytical methods that are non-simulation based and can be efficiently incorporated into iterative optimization algorithms to properly address the reliability benefits of wind DG by islanding.
- Gap 4: The optimization problem is mixed-integer, non-linear, and multi-objective due to the presence of continuous variables (DG sizes), integer variables (DG locations), and binary variables (switch states at different load levels). Although GWO has been used to solve similar problems, its basic form is prone to premature convergence and poor exploration capabilities in complex search spaces. There is a need for targeted modifications to enhance population diversity, exploration-exploitation tradeoffs, and convergence speed.

This paper fills these gaps by making the following contributions:

- Contribution 1 (Addressing Gaps 1 & 2): Formulation of a dual-objective stochastic model that optimizes wind DG allocation and load-level-dependent dynamic network reconfiguration under combined wind-load uncertainty, formulated as the Cartesian product of wind scenarios generated by PEM and different levels of loading.
- Contribution 2 (Addressing Gap 3): Inclusion of an analytical, simulation-free EENS calculation approach that takes into account the wind DG islanding capacity, allowing for efficient reliability analysis within the metaheuristic optimization framework.
- Contribution 3 (Addressing Gap 4): Presentation of the Improved Multi-Objective Grey Wolf Optimizer (I-MGWO) algorithm, which integrates three novel modifications tailored to this problem: (i) quasi-oppositional population initialization for enhanced initial diversity, (ii) adaptive stochastic coefficient approach that dynamically adjusts exploration-exploitation tradeoffs according to the fitness diversity of the population, and (iii) dynamic convex combination position update with global-best guidance for fast convergence.
- Contribution 4: Validation of the combined benefits of wind DG allocation and load-dependent reconfiguration far surpass the sum of individual improvements, with statistical analysis to confirm the significance of the findings.

To further clarify the novelty of this work relative to existing literature, Table 1 provides a systematic comparison of key features across representative studies. As shown in Table 1, the combination of features in this research study, namely: (i) joint optimization of wind DG and network reconfiguration based on load conditions, (ii) analytical calculation of EENS with islanding function, (iii) overall uncertainty modeling by Cartesian product of PEM scenarios and different load levels, and (iv) customized improved metaheuristic algorithm for this MIP stochastic problem, is a new contribution to the existing literature.

1.4 Paper Organization

The rest of the paper is organized as: Section 2 presents the uncertainty modeling and problem formulation, Section 3 explains the mathematical formulation, Section 4 describes the reliability evaluation methodology, Section 5 proposes the I-MGWO algorithm, Section 6 presents the simulation results, and finally Section 7 concludes the paper.

Table 1: Comparison of key features with existing literature.

Study	Wind Uncertainty	Load Levels	Network Reconfig.	DG Allocation	Reliability Objective	Analytical EENS	Multi-Objective	Simultaneous Optim.
Alanazi et al. [1]	✓ (PEM)	Single	✗	✓	✓	✗ (Simulation)	✓	N/A
Ahmed et al. [2]	✓ (Weibull)	Multiple	✗	✓	✗	N/A	✗	N/A
Zubair Iftikhar et al. [3]	✗	Multiple	✗	✓	✗	N/A	✓	N/A
Eid [9]	✗	Single	✗	✓	✗	N/A	✓	N/A
Salam et al. [13]	✗	Single	✗	✓	✓	✗ (Simulation)	✓	N/A
Júnior et al. [27]	✗	Single	✓	✓	✗	N/A	✓	✓
Cikan [29]	✗	Multiple	✓	✗	✓	✓	✓	N/A
This Work	✓ (PEM)	Multiple + Load-dependent reconfig.	✓ (load-dependent)	✓	✓	✓ (Analytical + Islanding)	✓	✓

2 Uncertainty Modeling for Wind Power Generation

The implementation of wind-based DG sources brings variability and uncertainty in a large way into the operations of a distribution network. Modeling of uncertainty in wind power output is critical in ensuring efficient network reconfiguration and allocation of wind DG sources with a focus on economy and feasibility. This takes place through a probabilistic model explained in this section [31,32].

2.1 Probabilistic Wind Speed Modeling

Wind speed is inherently stochastic and is commonly modeled using the Weibull distribution, which has been widely adopted in wind energy studies due to its flexibility in representing various wind regimes. The probability density function (PDF) of the Weibull distribution is given by [31,32]:

$$f(v \mid \lambda, k) = \left(\frac{k}{\lambda}\right)\left(\frac{v}{\lambda}\right)^{k-1} e^{-\left(\frac{v}{\lambda}\right)^{k}} \tag{1}$$

where v is the wind speed (m/s), k is the shape parameter (dimensionless), λ is the scale parameter (m/s).

The cumulative distribution function (CDF) is expressed as:

$$F(v) = 1 - e^{-\left(\frac{v}{\lambda}\right)^{k}} \tag{2}$$

Although the Weibull distribution serves as a parametric basis for wind speed modeling, the recent development of deep learning-based forecasting methods provides additional data-driven solutions that can be further utilized to improve the accuracy of wind speed forecasting. For example, the hybrid approach of Complete Ensemble Empirical Mode Decomposition with Adaptive Noise (CEEMDAN), Sample Entropy (SE), Variational Mode Decomposition (VMD), and Bidirectional Temporal Convolutional Network-Transformer (BiTCN-TR) has been shown to achieve better results in modeling the multi-scale temporal and non-stationary patterns of wind power time series [33]. The combination of data-driven wind speed forecasting models and the PEM-based scenario generation method may provide more accurate input

data for stochastic optimization, which can alleviate the conservatism of planning under uncertainty and potentially allow for higher wind penetration while meeting reliability criteria.

2.2 Wind Power Output Model

The electrical power output of a wind turbine is a function of wind speed and can be approximated using a piecewise linear model [22,31,32]:

$$P_w(v) = \begin{cases} 0 & \text{if } v \le v_{ci} \text{ or } v > v_{co} \\ P_r \cdot \dfrac{v - v_{ci}}{v_r - v_{ci}} & \text{if } v_{ci} < v \le v_r \\ P_r & \text{if } v_r < v \le v_{co} \end{cases} \tag{3}$$

where P_r is the rated power of the wind turbine, v_{ci} is the cut-in wind speed, v_r is the rated wind speed, and v_{co} is the cut-out wind speed.

2.3 Scenario Generation Using Point Estimation Method

To incorporate wind uncertainty into the optimization model, a scenario-based approach is employed using the Point Estimation Method (PEM). This method discretizes the continuous wind power distribution into a finite set of scenarios, each represented by a specific power output level and associated probability [31,32].

The steps for generating wind power scenarios are as follows:

- Determine boundary probabilities for zero and rated power outputs:

$$P_0 = \Pr\{P_w = 0\} = F(v_{ci}) + [1 - F(v_{co})] \tag{4}$$

$$P_r = \Pr\{P_w = P_r\} = F(v_{co}) - F(v_r) \tag{5}$$

- Define the conditional PDF for power output in the linear region ($v_{ci} \le v \le v_r$):

$$\tilde{f}_P(p) = \frac{f_v(v(p)) \cdot \dfrac{dv}{dp}}{1 - P_0 - P_r} \tag{6}$$

  where $v(p)$ is the inverse of the linear power-wind speed relationship.
- Compute statistical moments of the conditional distribution:
  Mean:

$$\mu_P = \int_0^{P_r} p \cdot \tilde{f}_P(p) dp \tag{7}$$

  Variance:

$$\sigma_P^2 = \int_0^{P_r} (p - \mu_P)^2 \cdot \tilde{f}_P(p) dp \tag{8}$$

  Central moments:

$$\lambda_j = \int_0^{P_r} \left(\frac{p - \mu_P}{\sigma_P} \right)^j \tilde{f}_P(p)\, dp, j = 3, 4 \tag{9}$$

- Solve for discrete points and weights using the moment matching equations:

$$\sum_{i=1}^{m} w_i \xi_i^j = \lambda_j, j = 1, \ldots, 4 \tag{10}$$

where ξ_i are the standardized locations and w_i are the corresponding weights. For a 5-point PEM, the locations and weights are calculated and presented in Section 6.

- Transform to actual power outputs and probabilities:

$$P_i = \mu_P + \sigma_P \cdot \xi_i \tag{11}$$

$$\pi_i = w_i \cdot (1 - P_0 - P_r) \tag{12}$$

The resulting set of power outputs $\{P_i\}$ with probabilities $\{\pi_i\}$, combined with the boundary points P_0 and P_r, form the discrete wind power scenario set used in the stochastic optimization model.

2.4 Integration with Load Uncertainty

In addition to wind power uncertainty, load variability is modeled using multiple loading levels (e.g., high, medium, low) based on typical daily or seasonal profiles. Each loading level is assigned to a duration factor, and the combined uncertainty space is constructed as the Cartesian product of wind scenarios and loading levels [22]. The coupling of stochastic wind modeling with network reconfiguration can be viewed as a topology-conscious approach to planning. In contrast to traditional planning approaches that assume the network topology to be fixed, the developed approach understands that optimal network performance under uncertainty can be achieved only through adaptive network topologies that are capable of adjusting to changing wind generation scenarios. This is in line with the latest flexibility-focused planning paradigms, where the network's capability to reconfigure its topology offers an additional degree of freedom to adapt to wind variability [22]. The Cartesian product formulation of the uncertainty space, which integrates wind scenarios with multiple levels of loading, allows the optimization problem to determine topology settings that are robust over the entire range of operating conditions, thus incorporating flexibility into the planning solution.

The proposed method of constructing scenarios based on the Cartesian product of discretized wind power scenarios and loading levels provides a computationally efficient solution compared to more complex stochastic programming models. Recent advances in coordinated renewable and flexibility resource management have considered different techniques for modeling uncertainties, such as: (i) robust optimization models that ensure feasibility for the worst-case scenario realization [1,23–25], (ii) chance-constrained models that enforce reliability constraints in a probabilistic manner [1,23–25], and (iii) distributionally robust models that account for ambiguity in the probability distributions [1,23–25]. In contrast to these models, our PEM-based scenario generation method strikes a balance between accuracy and computational efficiency, producing a discrete set of representative scenarios that retain the statistical moments of the original continuous distributions. This is particularly advantageous for the integration of metaheuristic optimization algorithms that require multiple objective function evaluations.

3 Problem Formulation

3.1 Introduction to the Optimization Framework

This paper proposes a dual-objective stochastic optimization approach to achieve the optimal allocation of wind-based DG in active distribution networks, considering network dynamic reconfiguration under multiple loading conditions. It seeks to find a set of Pareto-optimal solutions that will provide the best

trade-off between system energy losses reduction and system reliability enhancement. Although reductions in EENS and network energy losses may be positively correlated under certain operating conditions, they are not equivalent objectives. Loss minimization typically favors DG placement near load centers and low-impedance paths, whereas reliability enhancement (EENS reduction) promotes more spatially distributed DG placement to improve supply continuity during contingencies. Therefore, a Pareto-based multi-objective formulation is required to properly capture the trade-off between these objectives, rather than collapsing them into a single objective function. Unlike the commonly used single-objective methods, the proposed multi-objective formulation acknowledges the intrinsic conflict between technical performance and reliability. Thus, it allows decision makers to choose among the obtained solution according to the operational priorities. The overall structure of the proposed stochastic multi-objective framework is shown in Fig. 1.

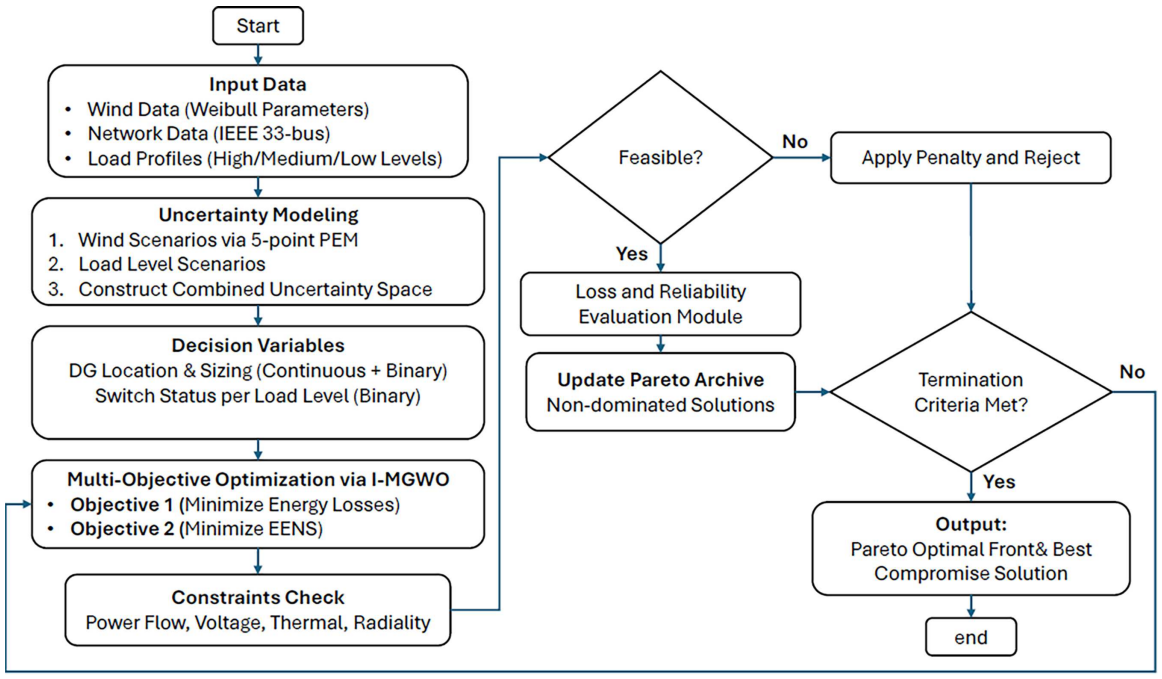

Figure 1: Overall flow of the proposed stochastic multi-objective framework for integrated wind DG allocation and network reconfiguration.

The multi-objective formulation is valid due to the conflict between the two objectives. Minimizing energy losses and maximizing reliability enhancement could be in conflict because the first objective might suggest DG placement near the load centers with low-impedance paths, while the second objective could require DG placement in a distributed manner to serve islanding during outages. The weighted sum method is not suitable for this trade-off because it requires assigning weights to the objectives, and it might not be able to identify the non-convex part of the Pareto front. The proposed multi-objective method is able to identify the entire Pareto front.

3.2 Modeling of Load Levels

The system load is represented by three different loading levels: High-H, Medium-M, and Low-L, which correspond to certain percentages of the peak load and for which specific annual duration is provided. That would ensure that the real consumption pattern in residential, commercial, and industrial categories is

represented accordingly in daily and seasonal variations [22]. Furthermore, the probabilities of each loading level are determined based on its annual duration about the total hours in a year.

Let LL be loading level index, $LL \in \{H, M, L\}$. Each loading level is featured by a load scaling factor λ^{LL}, which states the percentage of peak load, and by an annual duration T^{LL} in hours. In this way, the probability of each loading level may be calculated as:

$$\rho^{LL} = \frac{T^{LL}}{8760} \tag{13}$$

The active and reactive load at bus i for the loading level LL is calculated as:

$$P_i^{\text{load},LL} = \lambda^{LL} \cdot P_i^{\text{peak}} \tag{14}$$

$$Q_i^{\text{load},LL} = \lambda^{LL} \cdot Q_i^{\text{peak}} \tag{15}$$

It allows the optimization model to consider real load profiles for different operating conditions and, by doing so, enhances the practical relevance of the obtained solutions.

3.3 Objective Functions

3.3.1 Objective 1: Minimization of Total System Energy Losses

First, the objective function is directed at minimizing total energy losses in the distribution network. Energy losses are a serious economic and operational issue that distribution system operators face, as they lead to higher operational costs and decreased system efficiency [9,13]. By allocating wind DG at strategic points and dynamically reconfiguring the network, it is possible to minimize these losses, especially during high-load periods when such losses are greatest [22,27].

The expected annual energy losses are computed across all wind generation scenarios and loading levels, accounting for the probabilistic nature of wind power and load variability. This can be formulated as:

$$f_1 = E_{\text{Total}}^{\text{Loss}} = \sum_{s=1}^{N_s} \rho_s \cdot \sum_{LL=1}^{N_{LL}} \rho^{LL} \cdot \left[\sum_{(i,j)\in\Omega_{\text{line}}} r_{ij} \cdot I_{s,LL,ij}^2 \cdot T^{LL} \right] \tag{16}$$

In that equation, ρ_s represents the probability of wind scenario s; ρ^{LL} represents the probability of loading level LL. The term $r_{ij} \cdot I_{s,LL,ij}^2$ gives the resistive losses in line (i, j) under a specific wind scenario and loading condition. The inclusion of duration T^{LL} then turns the per-unit losses into annual energy losses, which provides a broad measure of system efficiency.

3.3.2 Objective 2: Enhancement of System Reliability

The second objective is to enhance the reliability of the distribution system, which is quantified by minimizing the EENS. As discussed, reliability is an important performance measure because interruptions to the power supply can cause economic losses and dissatisfaction on the part of consumers [13]. Wind DG can increase reliability due to localized generation at the time of faults or outages in cables/feeds, which reduces the effect of upstream failures on the downstream customers.

The total EENS is assessed over all wind scenarios and loading levels, inclusive of failure rates and repair times for the network components and the load demand at every bus. The objective function can be expressed as:

$$f_2 = \mathrm{EENS}_{\mathrm{Total}} = \sum_{s=1}^{N_s} \rho_s \cdot \sum_{LL=1}^{N_{LL}} \rho^{LL} \cdot \left[\sum_{i \in \Omega_{\mathrm{bus}}} C_i \cdot \mathrm{EENS}_{s,LL,i} \right] \tag{17}$$

where $\mathrm{EENS}_{s,LL,i}$ for bus i under scenario s and loading level LL is given by:

$$\mathrm{EENS}_{s,LL,i} = \sum_{k=1}^{N_{\mathrm{outages}}} \lambda_k \cdot r_k \cdot P_{s,LL,i}^{\mathrm{load}} \cdot \delta_{s,LL,i,k} \tag{18}$$

here, C_i denotes the cost of unsupplied energy at bus i, which can model economic impacts due to interruptions. The binary variable $\delta_{s,LL,i,k}$ equals 1 if bus i has an interruption by outage k for the given condition and thus links component failures to customer interruptions.

3.4 Power Flow Constraints

The distribution network operation should be satisfied with the fundamental laws of power flow for all considered scenarios and loading levels. Physical feasibility and operational stability are ensured with the following constraints.

The active power balance of each bus is maintained through Eq. (19), which considers power inflows, outflows, and losses:

$$P_{s,LL,i}^{\mathrm{net}} = \sum_{j \in \delta(i)} P_{s,LL,ij}^{\mathrm{line}} - \sum_{k \in \pi(i)} \left(P_{s,LL,ki}^{\mathrm{line}} - r_{ki} \cdot I_{s,LL,ki}^2 \right) + g_i \cdot V_{s,LL,i}^2 \tag{19}$$

Analogously, the balance of reactive power is imposed to guarantee voltage stability and adequate management of reactive power:

$$Q_{s,LL,i}^{\mathrm{net}} = \sum_{j \in \delta(i)} Q_{s,LL,ij}^{\mathrm{line}} - \sum_{k \in \pi(i)} \left(Q_{s,LL,ki}^{\mathrm{line}} - x_{ki} \cdot I_{s,LL,ki}^2 \right) + b_i \cdot V_{s,LL,i}^2 \tag{20}$$

The voltage drop equation, which includes both resistive and inductive effects, describes the relationship between voltage magnitudes at connected buses:

$$V_{s,LL,j}^2 = V_{s,LL,i}^2 - 2\left(r_{ij} \cdot P_{s,LL,ij}^{\mathrm{line}} + x_{ij} \cdot Q_{s,LL,ij}^{\mathrm{line}} \right) + \left(r_{ij}^2 + x_{ij}^2 \right) \cdot I_{s,LL,ij}^2 \tag{21}$$

Finally, apparent power flow constraint links current and voltage as well as flows in order to ensure coherence in the computation of power flows is expressed as follows:

$$I_{s,LL,ij}^2 \cdot V_{s,LL,i}^2 = \left(P_{s,LL,ij}^{\mathrm{line}} \right)^2 + \left(Q_{s,LL,ij}^{\mathrm{line}} \right)^2 \tag{22}$$

3.5 Network Operational Constraints

In this respect, several technical limits must be obeyed by the distribution network under all operating conditions to ensure safe and reliable operation.

Voltage magnitude at each bus should be within permissible limits to avoid damaging the equipment and to maintain power quality:

$$V_{\min} \le V_{s,LL,i}^2 \le V_{\max} \forall i \in \Omega_{\mathrm{bus}}, \forall s, \forall LL \tag{23}$$

Similarly, line currents cannot be in excess of their thermal ratings to prevent overheating and possible failure:

$$I^2_{s,LL,ij} \le I^2_{\max,ij} \forall (i,j) \in \Omega_{\text{line}}, \forall s, \forall LL \tag{24}$$

The net power injection at each bus is defined as the summation of wind DG output, existing DG contribution, and load demand:

$$P^{\text{net}}_{s,LL,i} = P^{\text{WDG}}_{s,LL,i} + P^{\text{DG}}_{s,LL,i} - P^{\text{load}}_{s,LL,i} \tag{25}$$

$$Q^{\text{net}}_{s,LL,i} = Q^{\text{WDG}}_{s,LL,i} + Q^{\text{DG}}_{s,LL,i} - Q^{\text{load}}_{s,LL,i} \tag{26}$$

3.6 Wind DG System Constraints

Wind DG integration at the distribution level must face several physical and operational constraints reflecting capabilities and limitations of the wind generation technology itself.

The active power output of a wind DG unit is bound by its installed capacity and the available wind resource, which varies by scenario and loading level:

$$0 \le P^{\text{WDG}}_{s,LL,i} \le P^{\text{WDG}}_{\text{rated},i} \cdot \gamma^{\text{wind}}_{s,LL} \cdot z^{\text{WDG}}_i \tag{27}$$

Practical considerations impose limits on the number and size of the wind DG that can be installed in the network. These are captured by the following constraints:

$$\sum_{i \in \Omega_{\text{bus}}} z^{\text{WDG}}_i \le N^{\max}_{\text{WDG}} \tag{28}$$

$$P^{\min}_{\text{WDG}} \cdot z^{\text{WDG}}_i \le P^{\text{WDG}}_{\text{rated},i} \le P^{\max}_{\text{WDG}} \cdot z^{\text{WDG}}_i \tag{29}$$

3.7 Network Reconfiguration Constraints

Network reconfiguration enables the dynamic modification of the network topology through opening and closing switches, thus providing a better load balancing and reduction of active power losses [27]. Therefore, this reconfiguration process has been modeled independently for each loading level to preserve the adaptative nature of modern distribution systems. The status of each line is modelled using a binary variable, where a value of one represents a line that is closed and conducting power:

$$\alpha^{LL}_{ij} \in \{0,1\} \forall (i,j) \in \Omega_{\text{line}}, \forall LL \tag{30}$$

To maintain the radial structure of the distribution network, which is a must for protection coordination and fault management, the number of closed lines must be one less than the number of buses:

$$\sum_{(i,j) \in \Omega_{\text{line}}} \alpha^{LL}_{ij} = N_{\text{bus}} - 1 \forall LL \tag{31}$$

Connectivity of the network is guaranteed by flow direction variables, which avoid the formation of isolated buses and ensure all the loads are supplied:

$$\beta^{LL}_{ij} + \beta^{LL}_{ji} = \alpha^{LL}_{ij} \forall (i,j) \in \Omega_{\text{line}}, \forall LL \tag{32}$$

$$\sum_{j \in \delta(i)} \beta^{LL}_{ij} = 1 \forall i \in \Omega_{\text{bus}} \backslash \{\text{substation}\}, \forall LL \tag{33}$$

Moreover, voltage feasibility needs to be guaranteed in any switching state to make sure that voltage limits are not violated no matter what the network topology is:

$$V_{s,LL,i}^2 \le V_{\max} \cdot \alpha_{ij}^{LL} + M \cdot (1 - \alpha_{ij}^{LL}) \tag{34}$$

$$V_{s,LL,i}^2 \ge V_{\min} \cdot \alpha_{ij}^{LL} - M \cdot (1 - \alpha_{ij}^{LL}) \tag{35}$$

4 Reliability Metrics Evaluation

4.1 Analytical Reliability Assessment Framework

In this section, a systematic methodology to assess the reliability of the distribution systems in terms of a particular calculation of EENS is introduced. As explained before, EENS represents the second objective function in our methodology. The strategy presented in this section allows an analytical calculation of reliability without simulative methods, which will make it efficient in terms of CPU time, taking into consideration that this calculation will need to be performed a large number of times during our search in optimized algorithms, such as those presented in future chapters.

The approach thematically integrates the uncertainty modeling of wind power generation presented in Section 2 and takes into consideration the reliability improvements achievable by wind DG under fault conditions because of localized generation as investigated in [34]. The approach considers realistic modeling of the support capability of wind resources for islanded mode operations, thus assessing in a realistic way the mitigation capacity achievable by strategic planning of wind DG in case of outages.

4.2 Expected Energy Not Supplied (EENS) Formulation

The EENS calculates repercussions of interruptions in terms of total energy not supplied to consumers based on all possible failure situations and their probabilistic chances in a way that restoration strategies incorporated in EENS are considered. The EENS model puts into focus both a probabilistic model of wind generation output in different scenarios, along with a multi-level load model.

The reliability objective function is formulated as:

$$f_2 = \mathrm{EENS}_{\mathrm{Total}} = \sum_{s=1}^{N_s} \rho_s \cdot \left[\sum_{LL=1}^{N_{LL}} \rho^{LL} \cdot \left(\sum_{i \in \Omega_{\mathrm{bus}}} P_{s,LL,i}^{\mathrm{load}} \cdot D_{s,LL,i}^{\mathrm{eff}} \right) \right] \tag{36}$$

where N_s is the total number of wind generation scenarios, ρ_s is the probability of wind scenario s (from Section 2), N_{LL} is the number of loading levels (High, Medium, Low), ρ^{LL} is the probability (duration fraction) of loading level LL, Ω_{bus} is the set of all buses in the network, $P_{s,LL,i}^{\mathrm{load}}$ is the load demand at bus i under scenario s and loading level LL, $D_{s,LL,i}^{\mathrm{eff}}$ is the effective annual interruption duration at bus i.

The effective interruption duration accounts for the reduction in outage time enabled by wind DG-supported island operation and is defined as follows [34]:

$$D_{s,LL,i}^{\mathrm{eff}} = DS_{s,LL,i} + (1 - \zeta_{s,LL,i}) \cdot (DR_{s,LL,i} - DS_{s,LL,i}) \tag{37}$$

where $DS_{s,LL,i}$ is the annual switching-only interruption duration (temporary outage during fault isolation), $DR_{s,LL,i}$ is the annual repair-and-switching interruption duration (outage requiring repair), and $\zeta_{s,LL,i}$ is the wind DG islanding capability indicator.

4.3 Radial Network Topology for Reliability Analysis

The core of reliability calculation relies on the radially connected network topology formed by the binary connectivity variables β_{ij}^{LL} presented in Section 3.7. The main idea of these variables is to represent the orientation of power flow and parent-child relationships among the buses, which make up an important part of calculating fault-propagation paths to the end consumers.

For each branch $(i, j) \in \Omega_{\text{line}}$, a binary variable β_{ij}^{LL} takes a value of 1 if the load bus j gets power from bus i for loading level LL, otherwise 0. The topology constraint for a radial system enforces each load bus, except for the "substation", to have exactly one "parent":

$$\sum_{j \in \delta(i)} \beta_{ij}^{LL} = 1 \forall i \in \Omega_{\text{bus}} \backslash \{\text{substation}\}, \forall LL \tag{38}$$

with this topological characteristic, a reliable analysis can be performed because it determines paths for each load bus. The failure of a component affects all buses below it, leaving all buses above unaffected. Such analysis makes it possible to recursively compute downtime in a systematic manner along each feeder.

4.4 Interruption Duration Calculations

4.4.1 Repair-and-Switching Interruption Duration

The length of a repair-and-switching interruption, $DR_{s,LL,j}$, is a function representing the interruptions that need both a switch and repair to affect a component. The value of this function is calculated recursively in a manner that begins at a substation and traverses a path radially [34].

For a bus j supplied by bus i (i.e., $\beta_{ij}^{LL} = 1$), the interruption duration is:

$$DR_{s,LL,j} = DR_{s,LL,i} + \Delta T_{ij} \cdot l_{ij} \cdot \lambda_{ij} \tag{39}$$

where $\Delta T_{ij} = TR_{ij} - TS_{ij}$ is the net repair duration for line (i, j), l_{ij} is the length of line (i, j) (km), λ_{ij} is the failure rate per unit length of line (i, j) (failures/km/year), TR_{ij} is the total repair time for line (i, j) (hours), and TS_{ij} is the switching time for line (i, j) (hours).

For buses directly connected to the substation, the initial interruption duration is:

$$DR_{s,LL,j} = TR_{ij} \cdot l_{ij} \cdot \lambda_{ij} \forall j \in \delta(\text{substation}) \tag{40}$$

4.4.2 Switching-Only Interruption Duration

The length of a switching-only interruption can be denoted by $DS_{s,LL,i}$ because it considers transitory interruptions in a network during fault selection and network restoration before carrying out repair work. The time is affected by branch failures that are downstream of bus i but are not on the path to bus i's main supply [34].

$$DS_{s,LL,i} = \sum_{(k,m) \in \Omega_{\text{line}}} \psi_{km}^{i,LL} \cdot TS_{km} \cdot l_{km} \cdot \lambda_{km} \tag{41}$$

In this case, $\psi_{km}^{i,LL}$ is a binary topology parameter taking on a value of 1 if line (k, m) belongs to the downstream path of bus 'i' and would lead to a 'switching-only' event if faulted, and 0 otherwise. The above parameter is calculated using other parameters 'β_{ij}^{LL}'.

4.5 Wind DG Islanding Capability Assessment

The DG islanding capability index $\zeta_{s,LL,i}$ will indicate if a bus can be self-powered by local winds in case of an outage upstream. The presence of this capability can greatly lower the actual outage duration if adequate wind power is available in the local area to satisfy local load.

The indicator is defined as:

$$\zeta_{s,LL,i} = \begin{cases} 1 & \text{if } P^{\text{WDG}}_{s,LL,i} \geq P^{\text{load}}_{s,LL,i} \cdot \xi \text{ and } z^{\text{WDG}}_i = 1 \\ 0 & \text{otherwise} \end{cases} \tag{42}$$

where $P^{\text{WDG}}_{s,LL,i}$ is the available wind DG generation at bus i under scenario s and loading level LL, $P^{\text{load}}_{s,LL,i}$ is the load demand at bus i, ξ is a security factor (typically 0.9–1.0) accounting for operational margins and reserve requirements, z^{WDG}_i is the binary decision variable indicating wind DG installation at bus i.

The available wind generation is determined using the scenario-based uncertainty model from Section 2:

$$P^{\text{WDG}}_{s,LL,i} = P^{\text{WDG}}_{\text{rated},i} \cdot \gamma^{\text{wind}}_{s,LL} \cdot z^{\text{WDG}}_i \tag{43}$$

where $\gamma^{\text{wind}}_{s,LL}$ is the scenario- and load-level-dependent wind power output factor.

4.6 Comprehensive EENS Calculation Procedure

The full procedure for EENS calculation for each candidate DG allocation and network configuration considered during the optimization consists of the following steps:

4.6.1 Radial Topology Identification

- Identify network connectivity and parent-child relationships based on the binary variables β^{LL}_{ij} derived from solving the power flow and reconfiguration problem described in Section 3.7.

4.6.2 Interruption Duration Calculation

- Calculate repair-and-switching times $DR_{s,LL,i}$ recursively from the substation to all load buses.
- Compute the switching-only times $DR_{s,LL,i}$ given the downstream branch failure using $\psi^{i,LL}_{km}$ parameter.

4.6.3 Wind DG Islanding Capability Evaluation

- Calculate available wind generation $P^{\text{WDG}}_{s,LL,i}$.
- Calculate islanding indicators $\zeta_{s,LL,i}$ based on available generation relative to load demand.

4.6.4 Effective Interruption Duration

For each bus, calculate the available time:

$$D^{\text{eff}}_{s,LL,i} = DS_{s,LL,i} + (1 - \zeta_{s,LL,i}) \cdot (DR_{s,LL,i} - DS_{s,LL,i}) \tag{44}$$

This expression takes into consideration the fact that when grid connection is feasible ($\zeta = 1$), the interruption time will be solely for the switching-only duration.

4.6.5 Scenario and Loading Level Aggregation

The weighted EENS can be calculated for all wind directions and load levels with their respective probabilities of ρ_s and ρ^{LL}. The obtained EENS value gives a complete and situation-conscious estimate of system level reliability, considering both network topology level reliability and the improvement achieved by allocating strategic wind DG with capabilities of islanding mode support. This analytical technique gives a reliable estimate of system level reliability in an accurate and optimized manner, making it suitable for implementation with a metaheuristic search algorithm, such as the Improved GWO, in which thousands of solution paths need to be evaluated during search.

5 The Proposed Improved Multi-Objective Grey Wolf Optimizer (I-MGWO)

The stochastic optimal wind DG allocation with systems configuration in a distribution network is a non-linear, complex, and multiple objective optimization problem. To successfully counter this problem, this paper proposes an I-MGWO technique. This technique adds a strategic designs modification of conventional GWO to counter the problem of increased sensitivity to population initialization, pre-mature convergence, and a poor balance between exploration and local search of solutions in a global search space in a deepened manner with a combination of following modifications.

5.1 Foundation: Standard Grey Wolf Optimizer (GWO)

The GWO algorithm is a swarm intelligence technique based on social hierarchy and hunting behavior of grey wolves [35]. The search space is organized in a social hierarchy with an alpha (α) individual symbolizing the global optimum solution. The beta (β) and delta (δ) denote the second and third best solutions, respectively, and all other solutions are omega (ω) candidates. The search strategy in this optimization algorithm is driven by α, β, and δ wolves in a three-step manner [35]:

Social Hierarchy and Encircling Prey: The wolves adjust their positions to surround their prey (the best-known solution). This strategy can be described using these equations:

$$\vec{D} = \mid \vec{C} \cdot \vec{X}_p(t) - \vec{X}(t) \mid \tag{45}$$

$$\vec{X}(t+1) = \vec{X}_p(t) - \vec{A} \cdot \vec{D} \tag{46}$$

here, t represents the current iteration, $\vec{X}$ symbolizes the position vector of a wolf, and $\vec{X}_p$ represents the position vector of a prey. The coefficient vectors $\vec{A}$ and $\vec{C}$ are calculated using the following equations:

$$\vec{A} = 2\vec{a} \cdot \vec{r}_1 - \vec{a}, \vec{C} = 2 \cdot \vec{r}_2 \tag{47}$$

where $\vec{r}_1, \vec{r}_2$ are random vectors in [0, 1]. The components of vector $\vec{a}$ linearly decrease from 2 to 0 in order to regulate exploration and exploitation trade-off.

Hunting: The hunting procedure is controlled by the α, β, and the ones who are assumed to have knowledge of where the prey can be found. The ω wolves will update their positions based on:

$$\vec{D}_\alpha = \mid \vec{C}_1 \cdot \vec{X}_\alpha - \vec{X} \mid, \quad \vec{D}_\beta = \mid \vec{C}_2 \cdot \vec{X}_\beta - \vec{X} \mid, \quad \vec{D}_\delta = \mid \vec{C}_3 \cdot \vec{X}_\delta - \vec{X} \mid$$
$$\vec{X}_1 = \vec{X}_\alpha - \vec{A}_1 \cdot \vec{D}_\alpha, \quad \vec{X}_2 = \vec{X}_\beta - \vec{A}_2 \cdot \vec{D}_\beta, \quad \vec{X}_3 = \vec{X}_\delta - \vec{A}_3 \cdot \vec{D}_\delta \tag{48}$$

$$\vec{X}(t+1) = \frac{\vec{X}_1 + \vec{X}_2 + \vec{X}_3}{3}$$

5.2 Proposed Algorithmic Enhancements

5.2.1 Quasi-Oppositional Population Seeding

In standard random initialization, a non-uniform population distribution might exist, which may overlook interesting areas in the search space. To promote a higher level of population diversity right from initialization, the I-MGWO algorithm adopts a strategy called Quasi-Oppositional Learning (QOL) [20]. In this strategy, not only is a random population P initiated, but a quasi-opposite population QOP is also formed. The quasi-opposite point $\hat{x}_i$ for a variable x_i in given bounds $[lb_i, ub_i]$ can be computed using this formula:

$$\hat{x}_i = \text{rand}(\frac{lb_i + ub_i}{2}, \overline{x}_i) \tag{49}$$

where $\overline{x}_i = lb_i + ub_i - x_i$ is called the opposite point, and rand(a, b) gives a random number in the uniform distribution $a \leq \text{rand}(a, b) \leq b$. The fittest solutions among $P \cup QOP$ are chosen to create the initial population for I-MGWO to have a better initialization point, which approximates the global optimum.

5.2.2 Adaptive Stochastic Coefficient Strategy

To improve exploration capabilities and escaping local optimum solutions, a new Adaptive Stochastic Coefficient named ASC is added in the I-MGWO algorithm. Based on this adaptive strategy, a variation in the calculation of the coefficient vector $\vec{C}$ is achieved with consideration of diversity based on fitness functions rather than random numbers alone. The revised formula for the distance vector is:

$$\vec{D} = \mid \phi(t) \cdot \vec{C} \cdot \vec{X}_p(t) - \vec{X}(t) \mid \tag{50}$$

where $\phi(t)$ is an adaptive factor defined as:

$$\phi(t) = 1 + \sigma_f(t) \tag{51}$$

In this case, $\sigma_f(t)$ represents the normalized standard deviation of a population's fitness values for a given iteration t. With a large $\sigma_f(t)$ reflecting a scattered population, $\phi(t)$ will increase, encouraging exploration. With a converging population and accordingly a small $\sigma_f(t)$ moving towards the goal, $\phi(t)$ will tend towards a value of 1, favoring exploitation.

5.2.3 Dynamic Convex Combination Position Update

The standard GWO's update of positions is performed through a simple average of positions proposed by α, β, and δ wolves. But this update strategy leads to slow and sometimes poor convergence. In addition, in I-MGWO, a Dynamic Convex Combination (DCC) strategy with adaptive weights allocated to α, β, and δ wolves based on their fitness function, along with a global-best guided term, is used for accelerated convergence.

The position update is redefined as:

$$\vec{X}(t+1) = \frac{w_\alpha \vec{X}_1 + w_\beta \vec{X}_2 + w_\delta \vec{X}_3}{w_\alpha + w_\beta + w_\delta} + \eta \cdot \vec{r}_3 \cdot (\vec{X}_{Gbest} - \vec{X}(t)) \tag{52}$$

where the weights $w_\alpha = 3, w_\beta = 2, w_\delta = 1$ prioritize the leaders. $\vec{X}_{Gbest}$ is the best global position found so far (archived from the Pareto front). $\vec{r}_3$ is a random vector in [0, 1]. η is a time-varying attenuation coefficient.

A strategy with DCC ensures that the impact of more fit leaders will be higher, along with a direct momentum term towards the historically best region, which improves convergence greatly.

5.3 Multi-Objective Mechanism and Fitness Evaluation

The conventional GWO algorithm is intended for single objective optimization. To address this problem which contains bi-objectives—minimizing energy loss function (f_1), and improving reliability function (f_2)—the I-MGWO algorithm incorporates an external archive and a Pareto selection approach [36]. With this approach, it is possible for the algorithm to search and store different non-dominated solutions simultaneously to construct a Pareto optimal front.

5.3.1 External Archive and Pareto Dominance

A boundless external archive $\mathcal{A}$ is used in order to store all non-dominated solutions obtained during search. A solution vector $\vec{x}_1$ is considered to dominate another solution vector $\vec{x}_2$ (denoted as $\vec{x}_1 \prec \vec{x}_2$) if both of the following conditions are met:

- The solution $\vec{x}_1$ is no worse than $\vec{x}_2$ in all objectives: $f_k(\vec{x}_1) \leq f_k(\vec{x}_2)$ for all $k = 1, 2$.
- The solution $\vec{x}_1$ is strictly better than $\vec{x}_2$ in at least one objective: $f_k(\vec{x}_1) < f_k(\vec{x}_2)$ for at least one k.

On each iteration, solutions in the population are evaluated, and new non-dominated solutions are compared against solutions in the archive. Solutions which are non-dominated with respect to solutions in the archive are added to the archive, and solutions in the archive which are now dominated by the new solutions will be removed from the archive.

5.3.2 Leader Selection Using Crowding Distance

In single objective GWO algorithm, α, β, and δ wolves are the 'top three' solutions. In a multi-objective problem where more solutions exist without being dominated, a different selection strategy is needed to pick up the leaders to direct the search. I-MGWO picks α, β, and δ from archive $\mathcal{A}$ using 'Crowding Distance' strategy to maximize diversity. The crowding distance of a solution gives an indication of how dense solutions are in a region around a solution. A higher crowding distance indicates a less dense region, which is better to have a spread Pareto front. The crowding distance calculation for each solution in $\mathcal{A}$ is done using this formula for each objective k:

- Sort the archive members based on their value for objective k.
- Set an infinite distance for the boundary solutions, which correspond to minimal and maximal function values.
- For all other intermediate solutions i, calculate:

$$CD_k(i) = \frac{f_k(i+1) - f_k(i-1)}{f_k^{max} - f_k^{min}} \tag{53}$$

where f_k^{max} and f_k^{min} denote the maximum and minimum values of objective k. Overall crowding distance of a solution is calculated by addition of individual distances of a solution with respect to all other objectives:

$$CD(i) = \sum_{k=1}^{3} CD_k(i) \tag{54}$$

- The leaders for the hunting phase are then selected as:

  α: The solution in $\mathcal{A}$ with the smallest f_1 value (emphasizing loss).

  β: The solution in $\mathcal{A}$ with the smallest f_2 value (emphasizing reliability).

  δ: The solution in $\mathcal{A}$ with the largest crowding distance (emphasizing diversity).

  This leader selection strategy ensures that the search is guided towards different regions of the Pareto front in each iteration.

5.3.3 Fitness Assignment: Weighted Chebyshev Scalarization

A fitness assignment strategy is mandatory in order to assess and compare candidate solutions during the selection and update of solutions in the archive. The I-MGWO algorithm utilizes a Weighted Chebyshev Scalarization strategy [37]. The fitness $F(\vec{x})$ of a candidate solution $\vec{x}$ is assigned with respect to a reference point $\vec{z}^* = (z_1^*, z_2^*)$, where z_k^* represents the best-known value for objective k.

$$F(\vec{x}) = \max_{k=1,2}\{\lambda_k \cdot \mid f_k(\vec{x}) - z_k^* \mid\} \tag{55}$$

The weights $\vec{\lambda} = (\lambda_1, \lambda_2)$ are adjusted in each iteration based on the current archive's density to search regions with less representation on the Pareto front. A small fitness function $F(\vec{x})$ corresponds to a better solution. An algorithm is guaranteed in which each Pareto optimal solution can be attained using a weight vector.

5.3.4 Constraint Handling

Wind DG allocation problem is tackled with many constraint considerations such as power flow, voltage, thermal, and so on, as defined in Section 3. The I-MGWO algorithm adopts a feasibility-first strategy with a dynamic punishment function to address the constraint problem. The obtained solutions are evaluated based on the criteria:

- A feasible solution will always be preferable to an infeasible solution.
- Between two feasible solutions, a solution with a better Pareto rank is always given preference.

  Between two infeasible solutions, a solution with smaller total constraint violation $\Theta(\vec{x})$ is preferable.

  The constraint violation is calculated as:

$$\Theta(\vec{x}) = \sum_i \max(0, g_i(\vec{x})) + \sum_j \mid h_j(\vec{x}) \mid \tag{56}$$

where $g_i(\vec{x})$ are inequality constraints and $h_j(\vec{x})$ are equality constraints.

5.4 The Complete I-MGWO Procedure for Wind DG Allocation

The step-by-step process of I-MGWO for solving the problem of optimized allocation of wind DG is explained below and shown in Fig. 2.

5.4.1 Initialization

- Set algorithm parameters: population size N, maximum iterations T_{max}, archive size.
- Create an initial population of wolves using a Quasi-oppositional Population Seeding technique (Section 5.2.1).

- Initialize the external archive $\mathcal{A}$ as empty.
- Perform power flow analysis and reliability evaluation procedure for each wolf (solution) to calculate objective functions (f_1, f_2) and constrain violations.

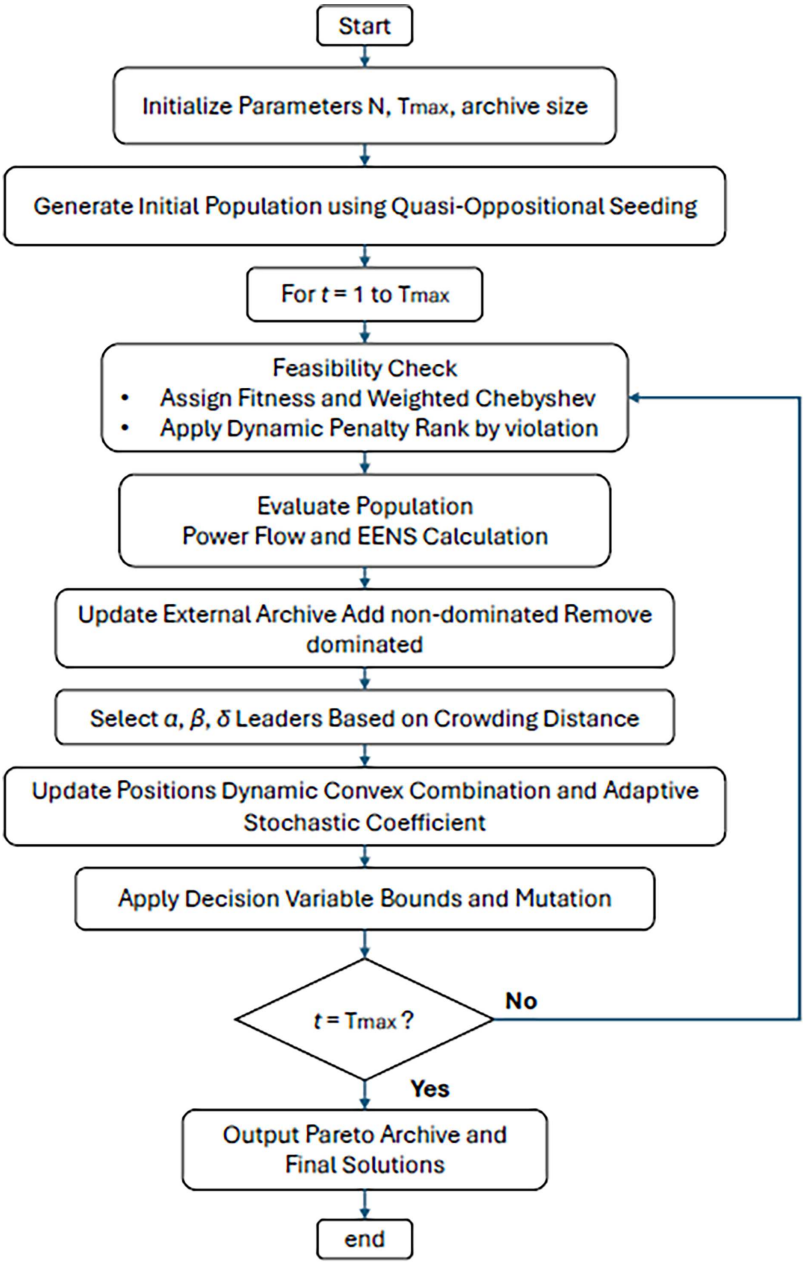

Figure 2: Flowchart of the proposed Improved Multi-Objective Grey Wolf Optimizer (I-MGWO).

5.4.2 Main Loop: For t = 1 to T_{max}

- Update Archive: Calculate the current population. Include all solutions not dominated in archive $\mathcal{A}$. Remove solutions from $\mathcal{A}$ if they are dominated.
- Select Leaders: With archive $\mathcal{A}$, pick leaders α, β, and δ using Crowding Distance strategy described in Section 5.3.2.

- Update Parameters: Compute a using both non-linear functions, which are the cosine control factor and w for DCC update.
- Update Positions: The update of positions for each wolf in the population using the Dynamic Convex Combination Subproblem (Section 5.2.3) and Adaptive Stochastic Coefficient Subproblem (Section 5.2.2).
- Apply Bounds: Make sure new solutions stay within feasible bounds for decision variables.
- Mutation: Use a low-probability mutation operator on a small population to maintain diversity. This operator serves as a secondary diversity mechanism, complementing the primary exploration provided by the adaptive stochastic coefficient strategy to enhance the algorithm's ability to escape local optima in highly non-linear search spaces.

5.4.3 Termination and Output

The algorithm ends when it attains a maximum total iteration T_{max}. The final output will be the non-dominated solutions computed in the external archive $\mathcal{A}$, which will represent the Pareto front for the wind DG allocation problem. A decision-making technique such as TOPSIS or Fuzzy satisfaction can be used on this front to identify the implementation strategy based on network preferences [38].

5.5 Theoretical Justification and Convergence Properties

The choice of the metaheuristic strategy for solving this problem is based on the nature of the wind DG allocation and network reconfiguration optimization problem:

1. Problem complexity: The problem has mixed-integer decision variables (continuous DG capacity, integer geographical location, and binary switch status at different load levels), non-linear power flow equations, and non-convex objective functions. Gradient-based optimization algorithms are not applicable because of the presence of discrete decision variables and non-convexities, and branch-and-bound algorithms are computationally infeasible for large problem sizes.
2. Stochastic objectives: The presence of uncertainty through scenario-based optimization leads to a stochastic objective function that needs to be aggregated over different scenarios. Metaheuristics are effective in solving such problems because they use only the objective function values to evaluate candidate solutions, without requiring gradient information or convexity.
3. Multi-objective nature: The requirement to find a wide range of Pareto-optimal solutions capturing trade-offs between energy losses and reliability makes the problem suited to population-based metaheuristics capable of exploring multiple areas of the solution space simultaneously.

In terms of convergence, although metaheuristics cannot ensure deterministic convergence to the global optimum, they can fulfill probabilistic convergence criteria under certain conditions. The original GWO algorithm has been proved to possess properties of Markov chains, and its convergence characteristics can be studied using the framework of stochastic processes [36]. The proposed modifications to I-MGWO maintain these theoretical underpinnings while offering improved performance:

- Quasi-oppositional seeding helps to enhance the initial distribution of the population within the search space, thus lowering the chances of premature convergence to local optima [20].
- The adaptive stochastic coefficient controls the exploration-exploitation tradeoff depending on population diversity. If the population is diverse (has high fitness variance), the exploration process is favored; otherwise, when the population becomes less diverse (indicating convergence), the exploitation process is strengthened. This adaptive process ensures the theoretical convergence property of the algorithm is retained, where it asymptotically converges to the Pareto optimal front without stagnation.

- The dynamic convex combination update with global-best support maintains the leader-following framework of GWO with faster convergence. The addition of the global-best component with a time-varying attenuation rate introduces elitism, which ensures that the best solutions are not discarded, meeting the convergence criteria of elitist multi-objective optimization algorithms [37].

It is worth pointing out that, in the context of NP-hard problems like the current ones, the aim is not to achieve global optimality (which is not computationally feasible for larger problem sizes) but to achieve high-quality approximate solutions within a reasonable computational time. The statistical results shown in Section 6.3.3 clearly show that I-MGWO performs significantly better in finding high-quality solutions in independent runs with very low standard deviations. The Friedman rank tests validate that the results are statistically significant.

6 Simulation Results and Discussion

6.1 System Data

6.1.1 Modeling of Wind Power Uncertainty

In order to model the wind generation as a stochastic input, the five-point estimation method is used, based on a Weibull distribution for the modeling of the wind speed. The parameters and resulting discrete distribution are given in Tables 2 and 3. The five-point estimation is a very effective method for the discretization of continuous wind power distribution, which captures the probabilistic nature of the wind generation without losing much computational efficiency in the stochastic optimization.

Table 2: Weibull distribution parameters and wind turbine specifications.

Parameter	Symbol	Value	Unit
Shape parameter	k	2	–
Scale parameter	λ	10	m/s
Cut-in wind speed	v_{ci}	3	m/s
Rated wind speed	v_r	15	m/s
Cut-out wind speed	v_{co}	25	m/s
Rated wind turbine power	P_r	2	MW

Table 3: Discrete wind power distribution scenario.

Scenario	Normalized Power Output (p.u.)	Probability	Description
1	0	0.088	Zero output (below cut-in/above cut-out)
2	0.1073	0.217	Low wind condition
3	0.4519	0.4038	Moderate wind condition
4	0.8503	0.1877	High wind condition
5	1	0.1035	Rated output

6.1.2 Load Level Modeling

Three different loading levels are considered in modeling the load demand that account for daily and seasonal variations. The properties of each of the loading levels considered are given in Table 4.

Table 4: Loading level characteristics.

Loading Level	Residential Load (% of Peak)	Commercial Load (% of Peak)	Industrial Load (% of Peak)	Annual Duration (hours)	Probability
High (H)	100%	100%	100%	2190	0.25
Medium (M)	57.50%	87.50%	79.00%	3650	0.417
Low (L)	30%	30%	72%	2920	0.333

The load at bus i for loading level LL is calculated as:

$$P_i^{load,LL} = \lambda_{LL}^{type} \cdot P_i^{peak} \tag{57}$$

where λ_{LL}^{type} is the load scaling factor for the specific load type (residential, commercial, or industrial) at the given loading level.

6.1.3 Constraints of Wind DG Allocation

A maximum of three wind DG units of the rated capacity of 2 MW each are permitted to be installed in the system. The candidate locations for wind DG installation are only load buses excluding the substation node. The optimization computes both the optimal locations (bus indices) and optimal capacities-0–2 MW per unit-for wind DG installation, with the constraint that at most three units may be installed. This considers practical limitations imposed by installation space availability, grid interconnection capacity, and investment budget constraints.

6.1.4 Network Reconfiguration Setup

The IEEE 33-bus system includes 5 normally open tie switches (lines 33–37) that can be operated to change the network topology. The reconfiguration optimization determines the optimal status (open/closed) of these switches for each loading level, subject to radiality and connectivity constraints as defined in Section 3.7. For independent operation at each loading level, the network topology can vary according to the different load conditions encountered during a year.

6.2 Case Studies

Four different operational cases are analyzed with the objective of understanding separate and integrated impacts of network reconfiguration and wind DG allocation. Each case identifies a different planning or operational strategy that might be followed by distribution system operators:

- Case 1 (Base Case): Original network configuration without wind DG or reconfiguration.
- Case 2: Reconfiguration Only: Network reconfiguration allowed without wind DG installation.
- Case 3 (Wind DG Only): Wind DG allocation allowed without network reconfiguration.
- Case 4: Combined Approach—Wind DG allocation integrated with network reconfiguration.

In this work, each case is analyzed for single-objective optimization-that is, minimizing energy losses or EENS separately-and multi-objective optimization, which minimizes both objectives simultaneously. Such a comprehensive analysis can allow deep comparison of different operational strategies and optimization approaches.

The optimization algorithms were run under identical computational conditions to ensure statistical robustness and a non-biased comparison. Each algorithm was run independently 25 times with a population size of 50 individuals and a maximum number of iterations of 100. Specific control parameters of the implemented algorithms in this study, namely the proposed Improved Grey Wolf Optimizer (IGWO), standard Grey Wolf Optimizer (GWO) [35], Particle Swarm Optimization (PSO) [39], and Genetic Algorithm (GA) [40] were set to their standard values as recommended in their original references, respectively, summarized in Table 5. This experimental setting provides a fair basis for testing the performance and reliability of algorithmic solutions across the four defined operational cases.

Table 5: Algorithm parameter settings for single-objective optimization.

Alg.	Key Parameters
IGWO	Quasi-oppositional factor, adaptive stochastic coefficient, dynamic convex combination weights ($w_\alpha = 3$, $w_\beta = 2$, $w_\delta = 1$), attenuation coefficient $\eta = 1 \rightarrow 0$
GWO	Convergence parameter a: linear decrease from 2 to 0; coefficients A, C as per standard equations
PSO	Inertia weight $w = 0.729$; cognitive coefficient c1 = 1.5; social coefficient c2 = 1.5
GA	Crossover probability = 0.8; mutation probability = 0.1; selection: tournament (size = 2)

The next subsections describe the specific results obtained for the minimization of total system energy losses and for the minimization of the EENS, analyzed individually. Values reported correspond to the best solution found in all 25 runs of each case.

6.3 Single-Objective Optimization Results

6.3.1 Energy Loss Minimization

Table 6 shows detailed results of the energy loss minimization problem for all cases and algorithms. The total annual energy losses in the base case, Case 1, amount to 742.89 MWh and set the baseline for comparing the performance of the different algorithms. In Case 2, where only reconfiguration is implemented, the loss reduction using the IGWO algorithm is the highest at 29.04%, bringing down total losses to 527.18 MWh. This represents the high potential that optimal network reconfiguration has in improving the efficiency of systems without the need for extra investment in generation. Case 3-wind DG only-presents even higher improvement possibilities, where the application of IGWO yielded a very impressive 50.20% energy loss reduction to 369.93 MWh. This huge improvement indicates that strategically placed wind DG is effective in minimizing line losses due to its localized generation. The most impressive results emerge in Case 4-IGWO, integrated approach, with maximum loss reduction of 55.70% (total losses reduced to 329.11 MWh). This synergy indeed confirms that the benefits from network reconfiguration and distributed generation allocation are complementary. Among all the cases, IGWO has always outperformed the conventional algorithms of standard GWO, PSO, and GA in energy loss minimization. In fact, the superiority of the algorithm is more distinct in the complicated Cases 3 and 4, where it shows superior convergence characteristic and high-quality solution.

Table 6: Optimal energy losses minimization results by different algorithms for cases.

Alg.	Load Level	Energy Loss (MWh)	EENS (MWh)	Min Voltage (p.u.)	Wind DG Locations	Wind P (MW)	Open Switches
Case 1							
base	1	456.53	19.38	0.91			33, 34, 35, 36, 37
	2	236.66	18.58	0.95			
	3	49.70	7.75	0.97			
	Total	742.89	45.71				
Case 2							
IGWO	1	321.35	17.41	0.94			33, 13, 10, 36, 37
	2	169.79	14.99	0.96			33, 34, 35, 14, 26
	3	36.04	6.01	0.98			33, 34, 10, 36, 28
	Total	527.18	38.42				
	Reduction (%)	29.04	15.96				
GWO	1	334.35	15.42	0.93			19, 13, 10, 17, 27
	2	176.01	12.29	0.96			7, 14, 10, 17, 26
	3	37.28	5.17	0.98			7, 13, 10, 17, 27
	Total	547.63	32.87				
	Reduction (%)	26.28	28.09				
PSO	1	456.53	20.62	0.91			20, 13, 10, 13, 22
	2	236.66	19.76	0.95			3, 12, 35, 17, 24
	3	49.70	8.25	0.97			5, 14, 21, 8, 5
	Total	742.89	48.62				
	Reduction (%)	0.00	−6.36				
GA	1	365.25	9.80	0.93			4, 12, 10, 15, 37
	2	191.72	10.52	0.96			4, 14, 18, 11, 28
	3	40.54	4.43	0.98			6, 13, 11, 17, 26
	Total	597.51	24.76				
	Reduction (%)	19.57	45.84				
Case 3							
IGWO	**Load Level**	**Energy Loss (MWh)**	**EENS (MWh)**	**Min Voltage (p.u.)**	**Wind DG Locations**	**Wind P (MW)**	**Open Switches**
	1	226.64	19.41	0.91	24, 30, 13	0.94, 0.70, 0.62	33, 34, 35, 36, 37
	2	113.88	18.60	0.95		0.50, 0.40, 0.38	
	3	29.41	7.65	0.97		0.52, 0.21, 0.16	
	Total	369.93	45.65				
	Reduction (%)	50.20	0.14				
GWO	1	251.25	18.46	0.91	30, 13, 32	0.60, 0.64, 0.08	33, 34, 35, 36, 37
	2	130.84	17.69	0.95		0.20, 0.39, 0.20	
	3	30.15	7.39	0.97		0.08, 0.09, 0.18	
	Total	412.24	43.54				
	Reduction (%)	44.51	4.75				
PSO	1	276.78	20.39	0.91	6, 14, 7	0.89, 0.41, 0.28	33, 34, 35, 36, 37
	2	129.14	19.54	0.95		0.82, 0.26, 0.12	
	3	37.78	8.15	0.97		0.47, 0.02, 0.37	
	Total	443.70	48.08				
	Reduction (%)	40.27	−5.17				

(Continued)

Table 6 (continued)

	1	286.89	19.84	0.91	11, 31, 24	0.41, 0.41, 0.43	33, 34, 35, 36, 37
	2	123.95	19.02	0.95		0.29, 0.41, 0.59	
GA	3	60.83	7.82	0.97		0.45, 0.42, 0.43	
		471.67	46.68				
	Reduction (%)	36.51	−2.12				
				Case 4			
IGWO	**Load Level**	**Energy Loss (MWh)**	**EENS (MWh)**	**Min Voltage (p.u.)**	**Wind DG Locations**	**Wind P (MW)**	**Open Switches**
	1	204.15	16.92	0.93	6, 2, 30	0.68, 0.67, 0.82	33, 9, 35, 36, 37
	2	100.15	17.39	0.96		0.45, 0.69, 0.58	33, 12, 35, 36, 37
	3	24.81	5.96	0.98		0.24, 0.32, 0.22	33, 34, 11, 17, 28
	Total	329.11	40.26				
	Reduction (%)	55.70	11.92				
	1	415.13	10.88	0.92	2	0.25	33, 9, 35, 6, 3
	2	215.55	10.43	0.95		0.24	33, 9, 35, 6, 3
GWO	3	45.45	5.69	0.98		0.09	33, 9, 35, 15, 26
	Total	676.14	27.00				
		8.99	40.93				
	1	293.32	14.02	0.92	32, 19, 26	0.94, 0.94, 0.30	33, 34, 35, 36, 3
	2	148.70	19.24	0.96		0.46, 0.73, 0.75	33, 34, 35, 36, 37
PSO	3	45.58	7.48	0.98		0.48, 0.00, 0.47	33, 34, 35, 36, 28
	Total	487.60	40.74				
	Reduction (%)	34.36	10.89				
	1	293.16	11.48	0.93	23, 11, 19	0.39, 0.20, 0.34	18, 13, 21, 8, 4
	2	151.24	9.99	0.96		0.41, 0.39, 0.24	3, 10, 8, 31, 26
GA	3	45.05	5.75	0.98		0.70, 0.39, 0.49	33, 34, 8, 36, 26
	Total	489.45	27.22				
	Reduction (%)	34.11	40.46				

6.3.2 EENS Minimization

The results on EENS minimization are summarized in Table 7, where the base case has an EENS of 45.71 MWh/year. However, in Case 2, IGWO gave the highest EENS reduction of 66.05% with a value of 15.52 MWh. It means that optimization of the supply paths and reducing outage impact due to network reconfiguration only can serve highly towards reliability improvement. In Case 3, the original GWO gives the best result: EENS is reduced by 8.66%, to 41.76 MWh-even then, this improvement is not as spectacular as in energy loss reductions. This suggests that wind DG allocation mainly improves energy efficiency without reconfiguration but does little to improve reliability. Case 4 gives the best result in IGWO for reliability enhancement, reaching a 61.41% reduction of EENS to 17.64 MWh. This significant enhancement confirms that the integrated approach of combining wind DG with network reconfiguration provides the richest reliability benefits.

Table 7: Optimal EENS minimization results by different algorithms for cases.

Alg.	Case 1						
	Load Level	Energy Loss (MWh)	EENS (MWh)	Min Voltage (p.u.)	Wind DG Locations	Wind P (MW)	Open Switches
base	1	456.53	19.38	0.91			33, 34, 35, 36, 37
	2	236.66	18.58	0.95			
	3	49.70	7.75	0.97			
	Total	742.89	45.71				
Alg.	**Case 2**						
IGWO	1	386.84	4.42	0.93			33, 13, 3, 6, 22
	2	202.81	4.53	0.96			33, 14, 3, 27, 23
	3	42.85	6.57	0.98			33, 13, 35, 17, 28
	Total	632.50	15.52				
	Reduction (%)	14.86	66.05				
GWO	1	495.85	10.36	0.92			7, 13, 11, 30, 25
	2	257.51	12.26	0.96			7, 13, 10, 17, 27
	3	54.12	5.94	0.98			18, 13, 10, 17, 25
	Total	807.48	28.56				
	Reduction (%)	−8.70	37.52				
PSO	1	495.05	5.15	0.91			3, 9, 35, 29, 22
	2	255.36	8.22	0.95			20, 34, 35, 25, 3
	3	53.47	4.18	0.98			7, 34, 35, 17, 3
	Total	803.88	17.55				
	Reduction (%)	−8.21	61.61				
GA	1	353.52	11.07	0.93			5, 34, 35, 8, 25
	2	185.41	5.74	0.96			6, 13, 11, 26, 23
	3	39.19	5.01	0.98			7, 12, 9, 16, 26
	Total	578.11	21.82				
	Reduction (%)	22.18	52.27				
Alg.	**Case 3**						
	Load Level	**Energy Loss (MWh)**	**EENS (MWh)**	**Min Voltage (p.u.)**	**Wind DG Locations**	**Wind P (MW)**	**Open Switches**
IGWO	1	307.02	18.13	0.91	30, 8, 32	0.19, 0.43, 0.44	33, 34, 35, 36, 37
	2	254.60	17.37	0.95		0.66, 0.27, 0.26	
	3	68.94	7.25	0.97		0.24, 0.23, 0.51	
	Total	630.56	42.75				
	Reduction (%)	15.12	6.49				
GWO	1	365.29	17.77	0.91	32, 25, 30	0.21, 0.12, 0.22	33, 34, 35, 36, 37
	2	179.36	17.03	0.95		0.43, 0.48, 0.28	
	3	67.78	6.96	0.97		0.06, 0.30, 0.39	
	Total	612.43	41.76				
	Reduction (%)	17.56	8.66				
PSO	1	296.47	18.36	0.91	32, 25, 8	0.75, 0.65, 0.39	33, 34, 35, 36, 37
	2	199.35	17.60	0.95		0.55, 0.47, 0.32	
	3	97.76	7.20	0.97		0.52, 0.77, 0.49	
	Total	593.58	43.16				
	Reduction (%)	20.10	5.59				

(Continued)

Table 7 (continued)

GA	1	330.80	18.28	0.91	25, 32, 24	0.38, 0.45, 0.36	33, 34, 35, 36, 37
	2	184.68	17.52	0.95		0.44, 0.44, 0.31	
	3	69.86	7.05	0.97		0.46, 0.42, 0.50	
	Total	585.34	42.85				
	Reduction (%)	21.21	6.27				
Alg.		**Case 4**					
	Load Level	**Energy Loss (MWh)**	**EENS (MWh)**	**Min Voltage (p.u.)**	**Wind DG Locations**	**Wind P (MW)**	**Open Switches**
IGWO	1	306.47	6.96	0.93	4, 33, 18	0.27, 0.32, 0.35	4, 11, 21, 26, 37
	2	162.29	4.65	0.96		0.41, 0.57, 0.37	4, 12, 35, 26, 22
	3	46.41	6.03	0.98		0.35, 0.48, 0.12	33, 9, 35, 36, 28
	Total	515.17	17.64				
	Reduction (%)	30.65	61.41				
GWO	1	408.02	10.88	0.92	2	0.1	33, 9, 35, 6, 3
	2	211.84	10.43	0.96	2	0.22	33, 9, 35, 6, 3
	3	44.21	6.03	0.98	2	0.28	33, 10, 35, 16, 26
	Total	664.07	27.34				
	Reduction (%)	10.61	40.20				
PSO	1	305.79	7.90	0.93	32, 30, 7	0.25, 0.73, 0.45	33, 34, 18, 7, 22
	2	184.84	6.16	0.96		0.21, 0.75, 0.67	33, 34, 3, 14, 23
	3	104.59	4.26	0.98		0.58, 0.21, 0.70	5, 34, 35, 16, 26
	Total	595.22	18.32				
	Reduction (%)	19.88	59.92				
GA	1	348.73	12.28	0.91	8, 20, 14	0.53, 0.51, 0.23	7, 12, 19, 9, 28
	2	182.70	7.20	0.95		0.61, 0.16, 0.19	6, 14, 11, 29, 22
	3	121.36	4.33	0.97		0.45, 0.27, 0.66	3, 34, 8, 13, 28
	Total	652.78	23.81				
	Reduction (%)	12.13	47.91				

6.3.3 Comparing Algorithm Performances

Voltage profiles from Figs. 3 and 4 show that voltage is within acceptable limits (0.91–0.98 p.u.) for all loading levels using both single-objective optimization approaches, while slightly better voltage profiles were provided by the energy loss minimization approach, since there was more effective power flow management.

Convergence characteristics as shown in Figs. 5 and 6 give insight into the superior performance of IGWO concerning convergence speed in all test cases. As one example, in Case 2, IGWO stabilizes near its optimum within about 20 iterations; however, PSO and GA need more than 75 iterations to approach convergence. In all Cases 3 and 4, IGWO also manages to reach a stable solution that is close to the optimum much more quickly than GWO, PSO, and GA do, hence proving its efficiency enhancement in solution space exploration. In terms of the final EENS minimization, IGWO tends to perform very well in most cases. This can be further elaborated by the fact that in Case 2, for example, IGWO yields the minimum total EENS value of 15.51886 MWh, as compared to GWO (28.56032 MWh), PSO (17.54883 MWh), and GA (21.81961 MWh). However, in Case 3, GWO gives the best final EENS of 41.75643 MWh, slightly better than that obtained by the IGWO (42.74620 MWh), PSO (43.15982 MWh), and GA (42.84960 MWh). Additionally, Case 4 indicates that IGWO, again, performed better with a total EENS value of 17.64064 MWh, while GWO, PSO, and GA deliver 27.33788, 18.32374, and 23.81452 MWh, respectively. The above results indeed reflect the fast convergence of the proposed IGWO algorithm and its strong overall performance; however, GWO may provide marginally better solutions in specific cases, such as Case 3.

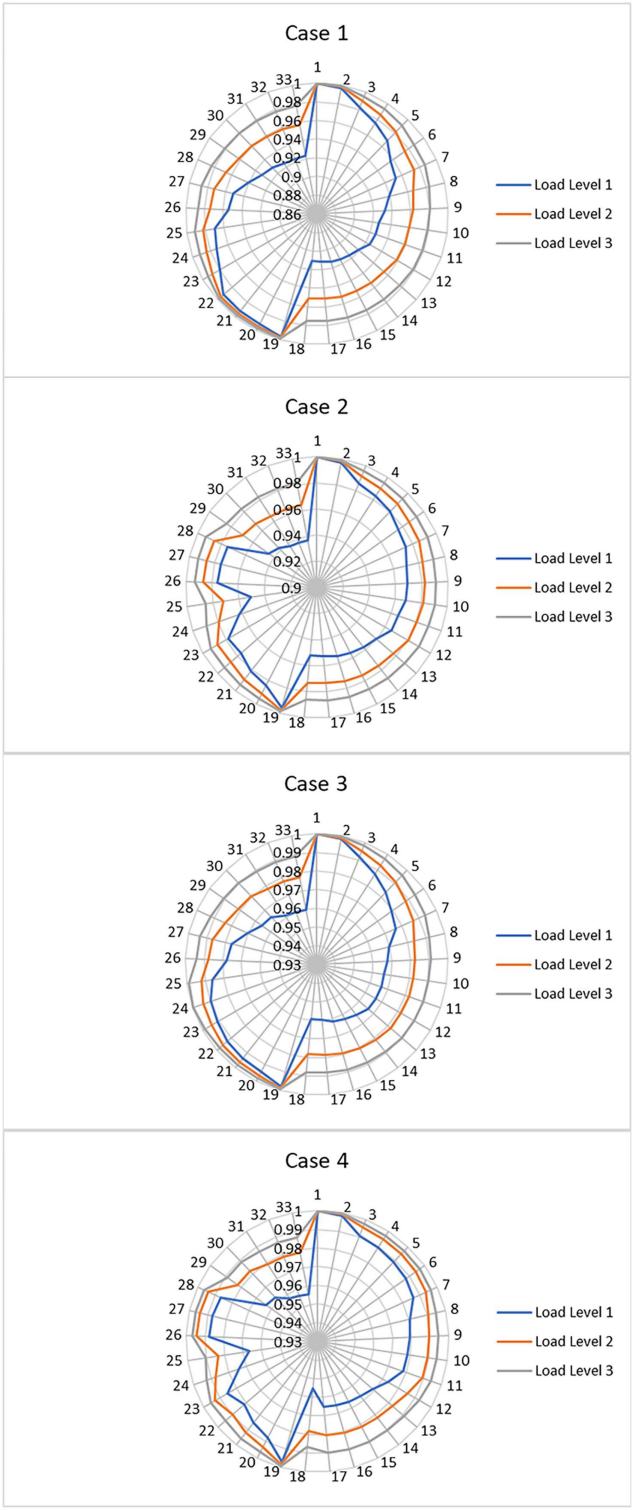

Figure 3: Voltage profiles of the IEEE 33-bus test system at different load levels-single objective energy loss minimization using IGWO.

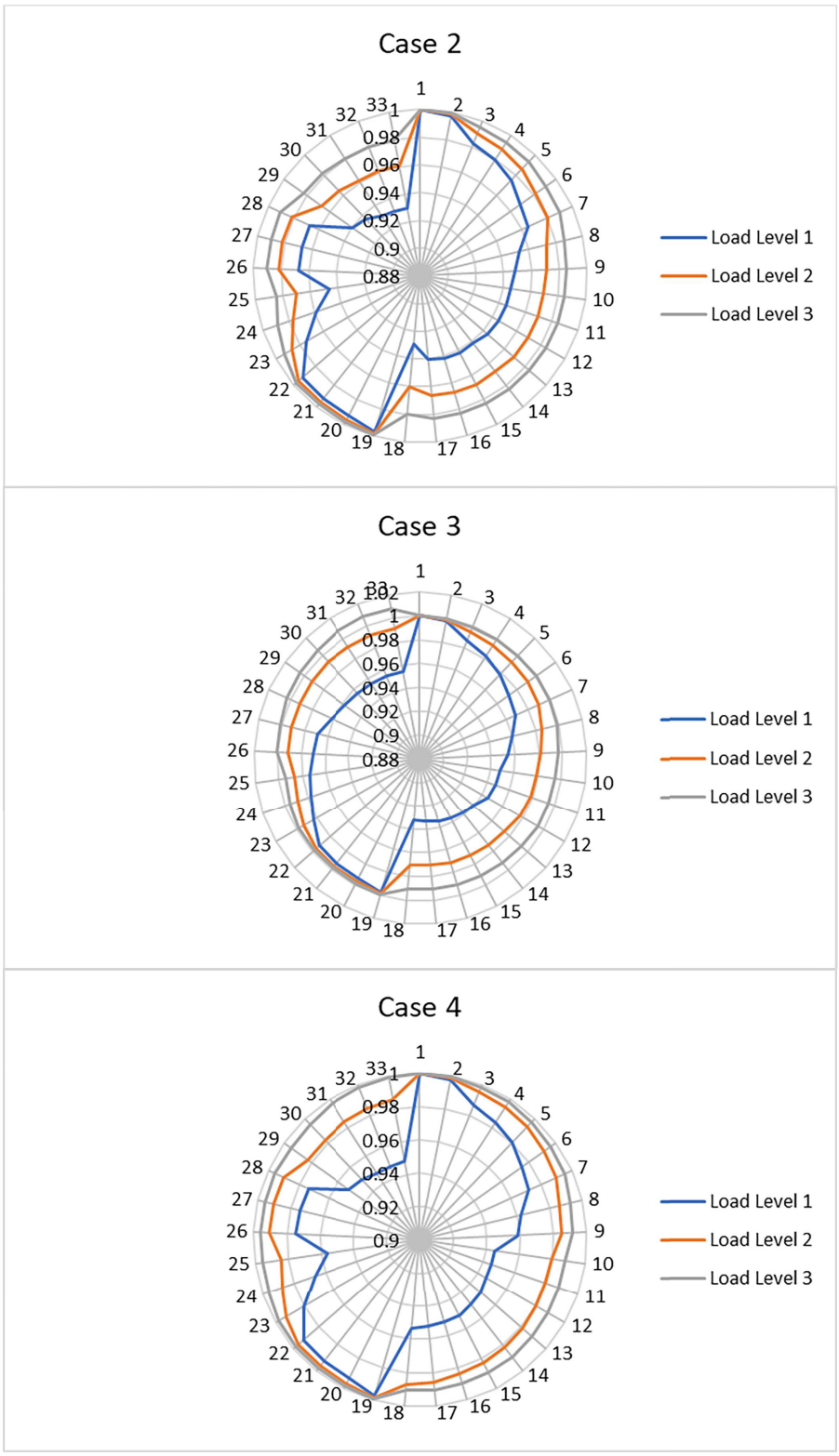

Figure 4: Voltage profiles of the IEEE 33-bus test system at different load levels-single objective EENS minimization using IGWO.

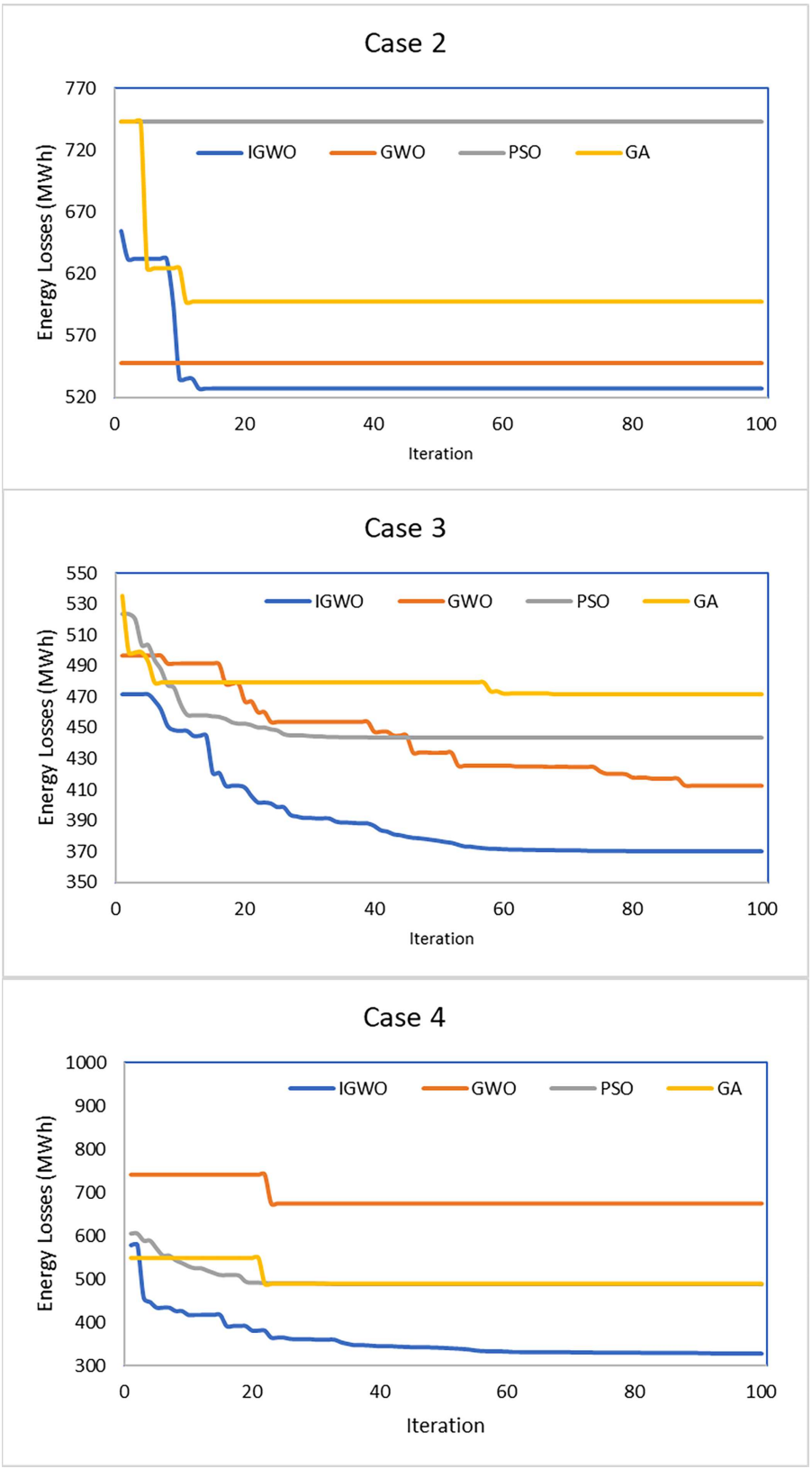

Figure 5: Convergence curves of the applied algorithms for single objective energy loss minimization problem.

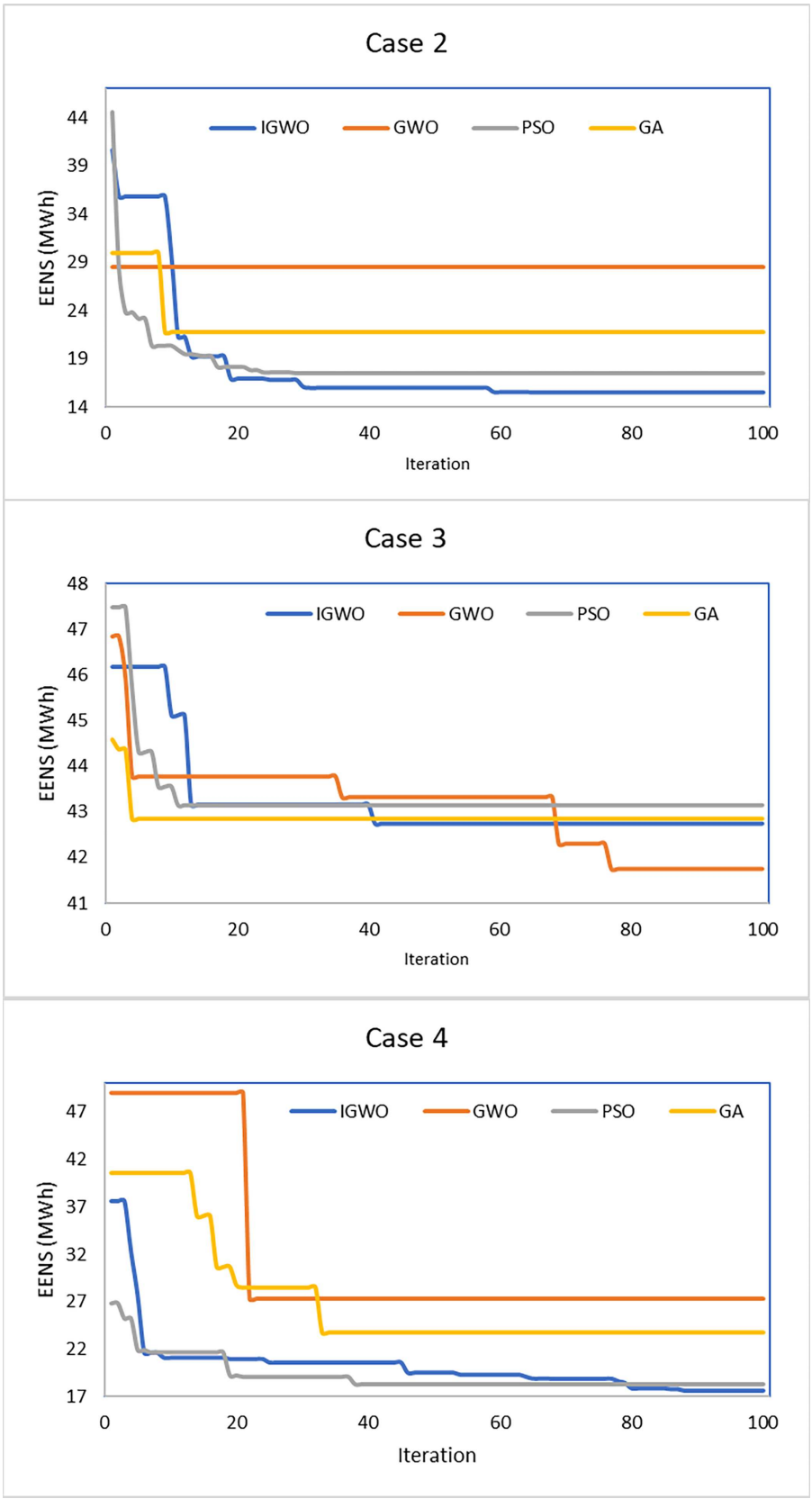

Figure 6: Convergence curves of the applied algorithms for single objective EENS minimization problem.

It is also important to note that the I-MGWO improvements incur some extra computational cost compared to the standard GWO. This is due to the fact that the quasi-oppositional seeding involves the evaluation of twice the population size during initialization (although only the best N are kept), and the computation of the crowding distance involves some extra operations per iteration proportional to the archive size. However, as shown in Figs. 5 and 6, the extra computational cost incurred by I-MGWO is offset by the improved search ability of I-MGWO, especially in the high-dimensional integrated Case 4, where the convergence difference between I-MGWO and standard GWO is most visible. The improved exploration abilities of the algorithm allow it to avoid premature convergence to local optima and explore better feasible solutions and move closer to the near-optimal regions compared to standard GWO. In terms of parameter settings, I-MGWO incurs a small number of additional parameters compared to standard GWO, although sensitivity analysis has shown that I-MGWO is less sensitive to the choice of initial parameters.

For statistical reliability, all algorithmic results were obtained from 25 independent runs to account for stochastic variability. The reported performance values in all tables correspond to the mean ± standard deviation over these runs. This inclusion of dispersion measures, together with the non-parametric Friedman and Bonferroni-corrected Wilcoxon tests, provides a consistent and statistically sound basis for comparison among algorithms, thereby improving the reproducibility and credibility of the conclusions. The statistical tests shown in Tables 8 to 10 confirm that IGWO has the best ranks according to all performance indicators. The low mean values obtained by the algorithm are associated with a low standard deviation (Tables 8 and 9), proving its quality and robustness. Based on the Friedman rank test for both objective functions and all cases, IGWO holds the first position.

Table 8: Energy loss statistics across all cases over 25 independent runs.

Case	Alg.	Mean ± Std. Dev. (MWh)	Minimum (MWh)	Friedman Rank	Performance vs. Base Case	Statistical Group
2	IGWO	537.18 ± 7.15	527.18	1	Best (27.7% improvement)	A (Superior)
2	GWO	592.87 ± 19.87	547.63	2	Good (20.2% improvement)	B
2	GA	622.18 ± 16.45	597.51	3	Moderate (16.3% improvement)	C
2	PSO	808.22 ± 11.32	742.89	4	Poor (−8.8% deterioration)	D
3	IGWO	376.84 ± 6.51	368.6	1	Best (49.3% improvement)	A (Superior)
3	GWO	464.52 ± 21.41	412.24	2.24	Very Good (37.5% improvement)	B
3	PSO	498.12 ± 19.84	443.7	2.96	Good (33.0% improvement)	C
3	GA	523.84 ± 21.56	471.67	3.8	Fair (29.5% improvement)	D

(Continued)

Table 8 (continued)

Case	Alg.	Mean ± Std. Dev. (MWh)	Minimum (MWh)	Friedman Rank	Performance vs. Base Case	Statistical Group
4	IGWO	336.84 ± 6.51	328.6	1	Best (54.7% improvement)	A (Superior)
4	PSO	522.12 ± 11.84	487.6	2.44	Good (29.7% improvement)	B
4	GA	525.84 ± 15.56	489.45	2.56	Good (29.2% improvement)	B
4	GWO	696.52 ± 14.41	676.14	4	Poor (6.2% improvement)	C

Table 9: EENS statistics across all cases over 25 independent runs.

Case	Algorithm	Mean ± Std. Dev. (MWh)	Minimum (MWh)	Friedman Rank	Performance vs. Base Case	Statistical Group
2	IGWO	18.14 ± 2.01	15.52	1	Best (60.3% improvement)	A (Superior)
2	PSO	21.84 ± 2.82	17.55	2	Very Good (52.2% improvement)	B
2	GA	29.12 ± 2.82	21.82	3	Good (36.3% improvement)	C
2	GWO	35.48 ± 3.37	28.56	4	Fair (22.4% improvement)	D
3	IGWO	43.27 ± 0.76	42.3	1.44	Best (5.3% improvement)	A (Superior)
3	GWO	43.46 ± 0.76	41.76	2.02	Very Good (4.9% improvement)	A-B
3	GA	43.85 ± 0.46	42.85	3.16	Good (4.1% improvement)	B-C
3	PSO	44.14 ± 0.61	43.16	3.38	Fair (3.4% improvement)	C
4	IGWO	18.14 ± 0.76	17.3	1.08	Best (60.3% improvement)	A (Superior)
4	PSO	19.04 ± 0.61	18.2	1.92	Excellent (58.3% improvement)	A-B
4	GA	25.22 ± 0.76	23.82	3	Good (44.8% improvement)	B
4	GWO	28.52 ± 0.61	27.34	4	Fair (37.6% improvement)	C

Table 10: Algorithm ranking summary for single objective optimization problems computed over 25 independent runs.

Rank	Energy Loss Minimization	EENS Minimization
1st	IGWO (All Cases)	IGWO (All Cases)
2nd	GWO (Cases 2, 3)/PSO (Case 4)	PSO (Cases 2, 4)/GWO (Case 3)
3rd	GA (Cases 2, 3)/GA (Case 4)	GA (Cases 2, 3, 4)
4th	PSO (Cases 2, 3)/GWO (Case 4)	GWO (Cases 2, 4)/PSO (Case 3)

To complement the Friedman test results already reported in Tables 8 and 9, a full post-hoc analysis was performed using the final 25-run datasets for all algorithms and cases. Pairwise Wilcoxon signed-rank tests were applied to determine which algorithms differ significantly in performance. Because four algorithms generate six pairwise comparisons, a Bonferroni-adjusted significance level of $\alpha_{adj} = 0.0083$ was used. The analysis was conducted separately for each case (2–4) and each objective (energy loss and EENS). This approach ensures a robust and statistically reliable comparison of IGWO against GWO, PSO, and GA on the realistic final simulation outputs.

The results of the Wilcoxon tests are summarized in Tables 11 and 12. For nearly all datasets across Cases 2–4, IGWO shows statistically significant superiority over all other algorithms. Only two comparisons failed to reach significance after Bonferroni correction: PSO vs. GA in Case 3 for EENS, and PSO vs. GA in Case 4 for energy loss. All remaining comparisons were significant. Combined with the Friedman statistics already presented in Tables 8 and 9, these findings provide strong and comprehensive statistical evidence that the proposed IGWO algorithm consistently outperforms the benchmark methods for both objectives across all case studies.

Table 11: Pairwise Wilcoxon signed-rank test results for energy loss (25 runs per algorithm, Bonferroni-adjusted significance level $\alpha_{adj} = 0.0083$).

Case	Comparison	Test Statistic	*p*-Value	Significant
Case 2	IGWO vs. GWO	0.0	5.96E−08	Yes
Case 2	IGWO vs. PSO	0.0	1.23E−05	Yes
Case 2	IGWO vs. GA	0.0	5.96E−08	Yes
Case 2	GWO vs. PSO	0.0	5.96E−08	Yes
Case 2	GWO vs. GA	0.0	5.96E−08	Yes
Case 2	PSO vs. GA	0.0	5.96E−08	Yes
Case 3	IGWO vs. GWO	0.0	5.96E−08	Yes
Case 3	IGWO vs. PSO	0.0	5.96E−08	Yes
Case 3	IGWO vs. GA	0.0	5.96E−08	Yes
Case 3	GWO vs. PSO	33.0	1.88E−04	Yes
Case 3	GWO vs. GA	0.0	5.96E−08	Yes
Case 3	PSO vs. GA	46.0	1.03E−03	Yes
Case 4	IGWO vs. GWO	0.0	5.96E−08	Yes
Case 4	IGWO vs. PSO	0.0	5.96E−08	Yes
Case 4	IGWO vs. GA	0.0	5.96E−08	Yes
Case 4	GWO vs. PSO	0.0	5.96E−08	Yes
Case 4	GWO vs. GA	0.0	1.23E−05	Yes
Case 4	PSO vs. GA	136.0	4.91E−01	No

Table 12: Pairwise Wilcoxon signed-rank test results for EENS (25 runs per algorithm, Bonferroni-adjusted significance level $\alpha_{adj} = 0.0083$).

Case	Comparison	Test Statistic	*p*-Value	Significant
Case 2	IGWO vs. GWO	0.0	1.20E−05	Yes
Case 2	IGWO vs. PSO	0.0	1.20E−05	Yes
Case 2	IGWO vs. GA	0.0	1.20E−05	Yes
Case 2	GWO vs. PSO	0.0	1.20E−05	Yes
Case 2	GWO vs. GA	0.0	1.20E−05	Yes
Case 2	PSO vs. GA	0.0	1.20E−05	Yes
Case 3	IGWO vs. GWO	34.0	2.60E−03	Yes
Case 3	IGWO vs. PSO	3.0	1.60E−05	Yes
Case 3	IGWO vs. GA	14.0	1.00E−04	Yes
Case 3	GWO vs. PSO	4.5	3.10E−05	Yes
Case 3	GWO vs. GA	35.5	3.08E−03	Yes
Case 3	PSO vs. GA	55.0	1.14E−02	No
Case 4	IGWO vs. GWO	0.0	1.20E−05	Yes
Case 4	IGWO vs. PSO	3.0	1.60E−05	Yes
Case 4	IGWO vs. GA	0.0	1.20E−05	Yes
Case 4	GWO vs. PSO	0.0	1.20E−05	Yes
Case 4	GWO vs. GA	0.0	1.20E−05	Yes
Case 4	PSO vs. GA	0.0	1.20E−05	Yes

6.4 Multi-Objective Optimization Results

The multi-objective optimization results manifest a complete view of trade-offs and synergistic effects between energy loss minimization and reliability enhancement (EENS reduction). All algorithms, such as MOIGWO and standard MOGWO [36], MOPSO [41], and NSGA-II [42], were executed with a population size of 50 and a maximum limit of iterations as 100 for fair comparison. The control parameters of competitive algorithms (MOGWO, MOPSO, NSGA-II) were set as per the standard values recommended in their respective foundational references to ensure a balanced and equitable performance assessment of all the algorithms.

Fig. 7 reports the Pareto fronts obtained by each compared metaheuristic. A comparison of the results clearly points out the different algorithmic behaviors. MOIGWO was able to produce the most spread out and widespread Pareto front in all the comparisons, with the highest Maximum Spread values in Cases 2 and 4, respectively, equal to 1.3245 and 1.2960. This means that it can explore the most extreme portions of the objective space. In addition, MOIGWO reached the best Hypervolume values in Cases 2 and 4, respectively, equal to 0.8916 and 0.8252, confirming that its solution set is not only diverse but also closer to the true Pareto-optimal front. NSGA-II showed an excellent spacing between solutions, especially in Cases 2 and 3 with SP values equal to 0.0378 and 0.0839. Nevertheless, considering the overall convergence, measured through HV, it generally resulted in being worse than that ensured by MOIGWO. MOGWO showed a good diversity in the population, but it got the poorest convergence with the worst HV values for each case. MOPSO has an incoherent trend, too often obtaining the smallest spread and the worst spacing, with the lowest ranking index. This explains why the Pareto fronts in Fig. 7 do not collapse to a single minimum point, even though the objectives may exhibit partial correlation.

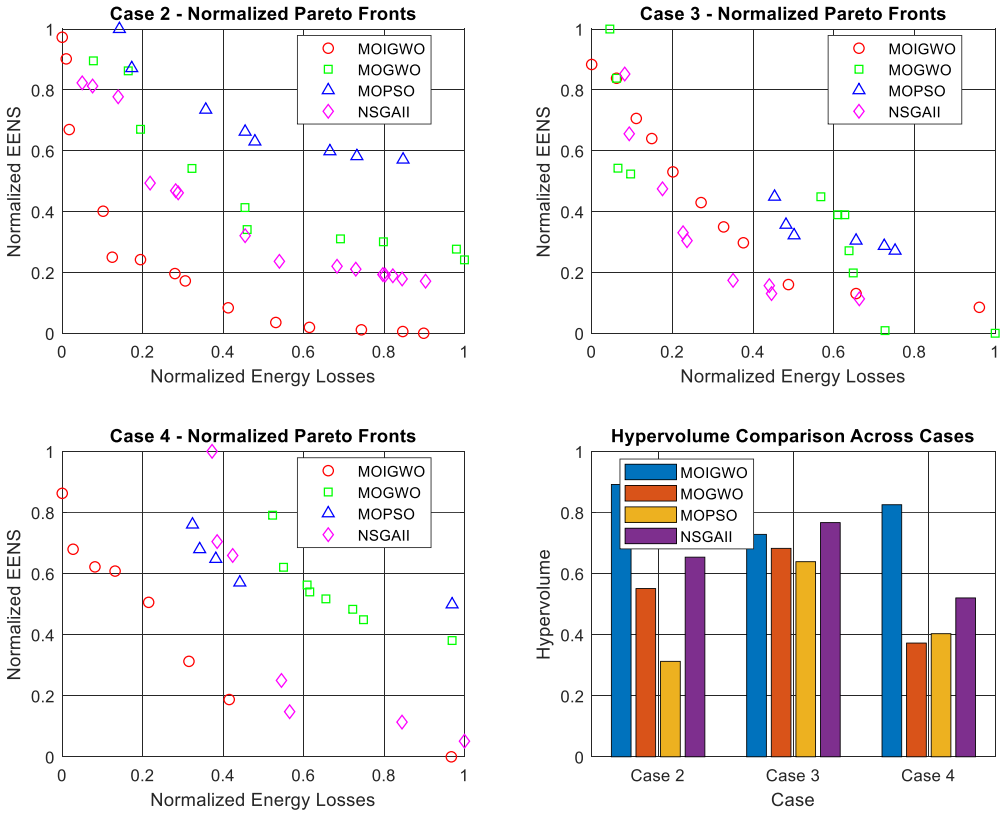

Figure 7: Pareto fronts obtained by multiobjective optimization algorithms.

The best compromise solutions, chosen from the Pareto front using a fuzzy decision-making method, are presented in Tables 13 and 14. These solutions provide the most balanced trade-off between the two conflicting objectives to achieve the maximum overall improvement with respect to the base case. MOIGWO found the most balanced compromise solutions in the integrated Case 4: this case yields a total improvement of 38.00% (31.35% loss reduction and 44.66% EENS reduction). MOIGWO was also able to provide the best overall solution for Case 2, yielding an overall gain of 38.50%. Additionally, for Case 3-Wind DG Only-a total gain of 21.66% was achieved by the best compromise solution offered by NSGA-II. This again points towards the very important implication of having only wind DG-based allocations, which decreases the energy losses significantly, but does not improve the reliability as much as it would with the adaptability provided by the network reconfiguration. Indeed, the compromises obtained for Case 4 outperform the results by Case 2 or Case 3 alone in terms of better/balanced improvements in both objectives, confirming that the co-optimization between generation placement and network topology benefits from synergies.

Table 13: Performance comparison table for multi-objective optimization model.

Algorithm	Maximum Spread (MS)	Spacing (SP)	Hypervolume (HV)	Overall Ranking
MOIGWO	Best in 2/3 cases Case 2: 1.3245 ✓ Case 3: 1.2491 Case 4: 1.2960 ✓	Variable performance Case 2: 0.0527 (3rd) Case 3: 0.0731 (2nd) Case 4: 0.1726 (worst)	Best in 2/3 cases Case 2: 0.8916 ✓ Case 3: 0.7283 Case 4: 0.8252 ✓	1st—Best overall

(Continued)

Table 13 (continued)

Algorithm	Maximum Spread (MS)	Spacing (SP)	Hypervolume (HV)	Overall Ranking
MOGWO [36]	Good spread Case 2: 1.1310 (2nd) Case 3: 1.3828 ✓ Case 4: 0.6062	Consistently good spacing Case 2: 0.0495 (2nd) Case 3: 0.0852 (3rd) Case 4: 0.0769 (2nd)	Lowest HV overall Case 2: 0.5507 (3rd) Case 3: 0.6825 (3rd) Case 4: 0.3724 (worst)	3rd—Good diversity, poor convergence
MOPSO [41]	Smallest spread Case 2: 0.8256 (worst) Case 3: 0.3474 (worst) Case 4: 0.6964	Poor spacing consistency Case 2: 0.0397 ✓ Case 3: 0.0266 ✓ Case 4: 0.2076 (worst)	Low-medium HV Case 2: 0.3126 (worst) Case 3: 0.6387 (worst) Case 4: 0.4030 (3rd)	4th—Inconsistent performance
NSGAII [42]	Consistent performance Case 2: 1.0741 (3rd) Case 3: 0.9404 (2nd) Case 4: 1.1376 ✓	Excellent spacing in 2/3 cases Case 2: 0.0378 ✓ Case 3: 0.0839 (worst) Case 4: 0.0828 ✓	Good convergence Case 2: 0.6536 (2nd) Case 3: 0.7666 ✓ Case 4: 0.5201 (2nd)	2nd—Most balanced algorithm

Table 14: Best compromise solutions comparison.

Case	Alg.	Energy Loss (MWh)	EENS (MWh)	Loss Imp. (%)	EENS Imp. (%)	Total Imp. (%)
2	MOIGWO	538	23.12	27.58	49.43	38.5
	MOGWO	625	24.25	15.87	46.95	31.41
	MOPSO	598.3	29.15	19.46	36.23	27.85
	NSGAII	580.54	25.75	21.85	43.67	32.76
3	MOIGWO	510	42.66	31.35	6.68	19.02
	MOGWO	430	43.96	42.12	3.84	22.98
	MOPSO	546	42.8	26.5	6.38	16.44
	NSGAII	470	42.7	36.73	6.59	21.66
4	MOIGWO	510	25.3	31.35	44.66	38
	MOGWO	570	28.4	23.27	37.88	30.58
	MOPSO	517.9	28.67	30.29	37.28	33.79
	NSGAII	555	24.95	25.29	45.42	35.36

6.5 Limitations and Practical Considerations

While the results reveal very promising potential for the proposed integrated framework, some practical limitations and implementation considerations are in order. The computational burden of the stochastic approach presents scalability challenges when applying the framework to larger distribution systems, as each additional bus increases the dimensionality of the search space and the complexity of power flow calculations, potentially leading to quadratic increases in computation time. In particular, the optimization model relies on perfect forecasting of wind power scenarios and deterministic load levels, while actual distribution system operations must deal with forecast errors and continuous rather than discretized load variations. In particular, the optimization model relies on perfect forecasting of wind power scenarios and deterministic load levels, while actual distribution system operations must deal with forecast errors and continuous rather than discretized load variations. This points to the need for robust or adaptive real-time strategies to

complement the offline planning solution. Furthermore, this work focuses on steady-state analysis and does not explicitly model transient stability and protection coordination challenges that may arise in dynamic network reconfiguration. The latter aspects are quite critical for practical implementation since switching operations need to be performed in a way that system stability is guaranteed and coordination among protective devices is maintained. Although the economic dimension has been recognized, it has not yet been completely included in the present technical optimization. The planning decision would necessitate a rigorous cost-benefit study that involves investment cost of wind DGs, switching operation and maintenance cost, and economic benefit due to improvements in reliability. The proposed model applied three fixed loading levels, which, though representative, simplifies real load profile continuous temporal variability. Higher time resolution such as hourly or daily segments may result in higher precision and more relevance to operation for the model but at greater computational complexity. The final assumption in the optimization is that all candidate buses and switches are indeed available for intervention, which might not be held true in practice because of physical constraints, land availability, or regulatory restrictions. These spatial and regulatory limitations should be part of future work with the aim of improving practical applicability based on the proposed methodology. In any case, the framework developed here provides a sound basis from a methodological point of view for strategic planning, where substantial technical benefits can be attained via coordinated wind DG allocation and network reconfiguration.

7 Conclusion

This paper presents the development and validation of an integrated stochastic multi-objective optimization framework for optimal allocation of wind-based DG in active distribution networks, which incorporates probabilistic modeling of wind uncertainty, multi-level load representation, and dynamic network reconfiguration. It attempts to tackle the two-fold objectives of energy loss minimization and system reliability improvement. The simulation conducted on the IEEE 33-bus system indicates that coordination of wind DG placement with adaptive network reconfiguration yields superior performance against implementing either of the two approaches. In a tabulated form, the key numerical findings are summarized below:

- The maximum reduction—55.7% in total annual energy losses and 61.4% in Expected Energy Not Supplied, was achieved for this integrated approach against the base case.
- The proposed Improved Multi-Objective Grey Wolf Optimizer outperformed the established algorithms concerning convergence speed, solution quality, and Pareto front diversity-Standard GWO, PSO, GA, and NSGA-II-reached the highest Hypervolume value of 0.8916 and Maximum Spread of 1.3245 in the critical test cases.
- In the multi-objective framework, the best compromise solution from the integrated case had a total improvement of 38.0%, balancing a 31.4% loss reduction with a 44.7% EENS reduction.

Mainly, the trade-offs between technical efficiency and reliability are stressed, along with the importance of multi-objective optimization in finding balanced Pareto-optimal solutions. Whereas the study acknowledges some practical limitations relating to forecast uncertainties and protection coordination details, the presented framework sets a sound methodological basis for distribution system planners who aim at fully exploiting renewable generation while preserving operational efficiency and reliability. Further research work will be aimed at extending the model by adding economic objectives, finer time resolutions, and real-time operational constraints.

Acknowledgement: The author extends the appreciation to the Deanship of Postgraduate Studies and Scientific Research at Majmaah University for funding this research work through the project number (R-2026-141).

Funding Statement: The author extends the appreciation to the Deanship of Postgraduate Studies and Scientific Research at Majmaah University for funding this research work through the project number (R-2026-141).

Availability of Data and Materials: Not applicable.

Ethics Approval: Not applicable.

Conflicts of Interest: The author declares no conflicts of interest.

References

1. Alanazi A, Alanazi M, Nowdeh SA, Abdelaziz AY, Abu-Siada A. Stochastic-metaheuristic model for multi-criteria allocation of wind energy resources in distribution network using improved equilibrium optimization algorithm. Electronics. 2022;11(20):3285. doi:10.3390/electronics11203285.
2. Ahmed A, Nadeem MF, Ali Sajjad I, Bo R, Khan IA. Optimal allocation of wind DG with time varying voltage dependent loads using bio-inspired: salp swarm algorithm. In: Proceedings of the 2020 3rd International Conference on Computing, Mathematics and Engineering Technologies (iCoMET); 2020 Jan 29–30; Sukkur, Pakistan. p. 1–7. doi:10.1109/icomet48670.2020.9074118.
3. Zubair Iftikhar M, Imran K, Imran Akbar M, Ghafoor S. Optimal distributed generators allocation with various load models under load growth using a meta-heuristic technique. Renew Energy Focus. 2024;49(4):100550. doi:10.1016/j.ref.2024.100550.
4. Ali A, Abbas G, Keerio MU, Mirsaeidi S, Alshahr S, Alshahir A. Pareto front-based multiobjective optimization of distributed generation considering the effect of voltage-dependent nonlinear load models. IEEE Access. 2023;11:12195–217. doi:10.1109/ACCESS.2023.3242546.
5. Al-Shamma'a AA, Farh HMH, Taiwo R, Ibrahim AW, Alshaabani A, Mekhilef S, et al. A comprehensive review of sizing and allocation of distributed power generation: optimization techniques, global insights, and smart grid implications. Comput Model Eng Sci. 2025;145(2):1303–47. doi:10.32604/cmes.2025.071302.
6. Kumar M, Soomro A, Uddin W, Kumar L. Optimal multi-objective placement and sizing of distributed generation in distribution system: a comprehensive review. Energies. 2022;15(21):7850. doi:10.3390/en15217850.
7. Kerur P, Keerthi Kumar SH, Prakash MN. A review and comparative study on different algorithms in efficient DG allocation in power distribution networks. In: Proceedings of the 2025 5th International Conference on Intelligent Technologies (CONIT); 2025 Jun 20–22; Hubbali, India. p. 1–9. doi:10.1109/CONIT65521.2025.11167763.
8. Akbar MI, Ali Abbas Kazmi S, Alrumayh O, Khan ZA, Altamimi A, Malik MM. A novel hybrid optimization-based algorithm for the single and multi-objective achievement with optimal DG allocations in distribution networks. IEEE Access. 2022;10:25669–87. doi:10.1109/ACCESS.2022.3155484.
9. Eid A. Allocation of distributed generations in radial distribution systems using adaptive PSO and modified GSA multi-objective optimizations. Alex Eng J. 2020;59(6):4771–86. doi:10.1016/j.aej.2020.08.042.
10. Pamshetti VB, Zhang W. Combined allocation of renewable-based distributed generation and soft open point into distribution networks in presence of plug-In electric vehicles: a multi-objective framework. In: Proceedings of the 2024 IEEE 4th International Conference on Sustainable Energy and Future Electric Transportation (SEFET); 2024 Jul 31–Aug 3; Hyderabad, India: IEEE. p. 1–6. doi:10.1109/SEFET61574.2024.10718231.
11. Saurav PK, Islam J, Borah P, Mansani S, Kayal P. Allocation and performance assessment of dispatchable distributed generators with multi-objective planning criteria. In: Proceedings of the 2023 IEEE 3rd International Conference on Smart Technologies for Power, Energy and Control (STPEC); 2023 Dec 10–13; Bhubaneswar, India. p. 1–6. doi:10.1109/STPEC59253.2023.10430599.
12. Prasad KRKV, Kollu R, Tiwari SK. An optimal multi-objective approach for distributed generation and AVR placement in distribution networks using IPMBSA. Electr Power Compon Syst. 2023;51(15):1523–45. doi:10.1080/15325008.2023.2199754.
13. Salam IU, Yousif M, Numan M, Zeb K, Billah M. Optimizing distributed generation placement and sizing in distribution systems: a multi-objective analysis of power losses, reliability, and operational constraints. Energies. 2023;16(16):5907. doi:10.3390/en16165907.

14. Zellagui M, Belbachir N, El-Sehiemy RA, El-Bayeh CZ. Multi-objective optimal allocation of hybrid photovoltaic distributed generators and distribution static var compensators in radial distribution systems using various optimization algorithms. J Electr Syst. 2024;18(1). doi:10.52783/jes.62.
15. He G, Su R, Yang J, Huang Y, Chen H, Zhang D, et al. Optimal location and sizing of distributed generator via improved multi-objective particle swarm optimization in active distribution network considering multi-resource. Energy Eng. 2023;120(9):2133–54. doi:10.32604/ee.2023.029007.
16. Gebril AM, Abd el-Ghany HA, Ali GEM, Zalhaf AS. Comprehensive framework for optimal distributed generation allocation in unbalanced distribution networks using genetic-algorithm. In: Proceedings of the 2024 25th International Middle East Power System Conference (MEPCON); 2024 Dec 17–19; Cairo, Egypt. p. 1–7. doi:10.1109/MEPCON63025.2024.10850047.
17. Elseify MA, Hashim FA, Hussien AG, Kamel S. Single and multi-objectives based on an improved golden jackal optimization algorithm for simultaneous integration of multiple capacitors and multi-type DGs in distribution systems. Appl Energy. 2024;353(3):122054. doi:10.1016/j.apenergy.2023.122054.
18. Eid A, El-Kishky H. Multi-objective Archimedes optimization algorithm for optimal allocation of renewable energy sources in distribution networks. In: Digital technologies and applications. Cham, Switzerland: Springer International Publishing; 2021. p. 65–75. doi:10.1007/978-3-030-73882-2_7.
19. Ebrahim MA, Ahmed EE, Salama MM, Ahmed MMR. Multi-objective optimization for optimum distributed generation integration in distribution networks. In: Proceedings of the 2024 25th International Middle East Power System Conference (MEPCON); 2024 Dec 17–19; Cairo, Egypt. p. 1–8. doi:10.1109/MEPCON63025.2024.10850254.
20. Taheri SI, Davoodi M, Ali MH. A simulated-annealing-quasi-oppositional-teaching-learning-based optimization algorithm for distributed generation allocation. Computation. 2023;11(11):214. doi:10.3390/computation11110214.
21. Chowdhury A, Roy R, Mandal KK. Optimal allocation of wind based DG for enhancement of technical, economic and social benefits using Jaya algorithm for radial distribution networks. In: Proceedings of the 2020 International Conference on Convergence to Digital World-Quo Vadis (ICCDW); 2020 Feb 18–20; Mumbai, India. p. 1–6. doi:10.1109/iccdw45521.2020.9318659.
22. Ehsanbakhsh M, Sepasian MS. Simultaneous siting and sizing of Soft Open Points and the allocation of Tie switches in active distribution network considering network reconfiguration. IET Gener Transm Distrib. 2023;17(1):263–80. doi:10.1049/gtd2.12683.
23. Saurav PK, Mansani S, Kayal P. Allocation of PV, wind, and biomass units with the multi-objective approach in an unbalanced power delivery network considering load and power generation uncertainty. In: Proceedings of the 2024 IEEE 4th International Conference on Sustainable Energy and Future Electric Transportation (SEFET); 2024 Jul 31–Aug 3; Hyderabad, India. p. 1–6. doi:10.1109/SEFET61574.2024.10718009.
24. Davoudkhani I, Zishan F, Mansouri S, Abdollahpour F, Grisales-Noreña L, Montoya O. Allocation of renewable energy resources in distribution systems while considering the uncertainty of wind and solar resources via the multi-objective salp swarm algorithm. Energies. 2023;16(1):474. doi:10.3390/en16010474.
25. Taha HA, Alham MH, Youssef HKM. Multi-objective optimization for optimal allocation and coordination of wind and solar DGs, BESSs and capacitors in presence of demand response. IEEE Access. 2022;10(3):16225–41. doi:10.1109/ACCESS.2022.3149135.
26. Tarraq A, El Mariami F, Belfqih A. Multi-objective distributed generation integration in radial distribution system using modified neural network algorithm. Int J Electr Comput Eng IJECE. 2023;13(5):4810. doi:10.11591/ijece.v13i5.pp4810-4823.
27. Júnior VFS, Ferraz RSF, Ferraz RSF, Rueda-Medina AC. Network reconfiguration and distributed generators allocation and sizing using multi-objective optimization algorithms. In: Proceedings of the 2023 15th Seminar on Power Electronics and Control (SEPOC); 2023 Oct 22–25; Santa Maria, Brazil. p. 1–6. doi:10.1109/SEPOC58810.2023.10322616.
28. Liu J, Zeng P, Li Y, Xing H. Coordinated optimal allocation of distributed generations in smart distribution grids considering active management and contingencies. J Electr Eng Technol. 2020;15(5):1969–83. doi:10.1007/s42835-020-00462-1.

29. Cikan M. Multi-objective approaches for optimizing 37-bus power distribution systems with reconfiguration technique: from unbalance current & voltage factor to reliability indices. Comput Model Eng Sci. 2025;143(1):673–721. doi:10.32604/cmes.2025.061699.
30. Song T, Teh J, Alharbi B. Reliability impact of dynamic thermal line rating and electric vehicles on wind power integrated networks. Energy. 2024;313:133945. doi:10.1016/j.energy.2024.133945.
31. Fu Q, Yu D, Ghorai J. Probabilistic load flow analysis for power systems with multi-correlated wind sources. In: Proceedings of the 2011 IEEE Power and Energy Society General Meeting; 2011 Jul 24–28; Detroit, MI, USA. p. 1–6. doi:10.1109/PES.2011.6038992.
32. Wen S, Lan H, Fu Q, Yu DC, Zhang L. Economic allocation for energy storage system considering wind power distribution. IEEE Trans Power Syst. 2015;30(2):644–52. doi:10.1109/TPWRS.2014.2337936.
33. Shi J, Teh J, Lai CM. Wind power prediction based on improved self-attention mechanism combined with bi-directional Temporal Convolutional Network. Energy. 2025;322(2):135666. doi:10.1016/j.energy.2025.135666.
34. Alanazi M, Alanazi A, Akbari MA, Deriche M, Ali Memon Z. A non-simulation-based linear model for analytical reliability evaluation of radial distribution systems considering renewable DGs. Appl Energy. 2023;342(4):121153. doi:10.1016/j.apenergy.2023.121153.
35. Mirjalili S, Mirjalili SM, Lewis A. Grey wolf optimizer. Adv Eng Softw. 2014;69:46–61. doi:10.1016/j.advengsoft.2013.12.007.
36. Mirjalili S, Saremi S, Mirjalili SM, dos S Coelho L. Multi-objective grey wolf optimizer: a novel algorithm for multi-criterion optimization. Expert Syst Appl. 2016;47(6):106–19. doi:10.1016/j.eswa.2015.10.039.
37. Kasimbeyli R, Ozturk ZK, Kasimbeyli N, Yalcin GD, Erdem BI. Comparison of some scalarization methods in multiobjective optimization. Bull Malays Math Sci Soc. 2019;42(5):1875–905. doi:10.1007/s40840-017-0579-4.
38. Wang Z, Rangaiah GP. Application and analysis of methods for selecting an optimal solution from the Pareto-optimal front obtained by multiobjective optimization. Ind Eng Chem Res. 2017;56(2):560–74. doi:10.1021/acs.iecr.6b03453.
39. Kennedy J, Eberhart R. Particle swarm optimization. In: Proceedings of the Proceedings of ICNN'95—International Conference on Neural Networks; 1995 Nov 27–Dec 1; Perth, WA, Australia. p. 1942–8. doi:10.1109/ICNN.1995.488968.
40. Holland JH. Genetic algorithms. Sci Am. 1992;267(1):66–72. doi:10.1038/scientificamerican0792-66.
41. Coello Coello CA, Lechuga MS. MOPSO: a proposal for multiple objective particle swarm optimization. In: Proceedings of the 2002 Congress on Evolutionary Computation CEC'02; 2002 May 12–17; Honolulu, HI, USA. p. 1051–6. doi:10.1109/CEC.2002.1004388.
42. Deb K, Pratap A, Agarwal S, Meyarivan T. A fast and elitist multiobjective genetic algorithm: NSGA-II. IEEE Trans Evol Comput. 2002;6(2):182–97. doi:10.1109/4235.996017.